Lattice gauge theory with Rydberg atoms.

Yannick Meurice

The University of Iowa
QuLAT collaboration
yannick-meurice@uiowa.edu
Supported by the Department of Energy under Award Number DOE DE-SC0019139 and DE-SC0010113

ECT Trento, June 6 2023

Students and postdocs

Research Group at U. Iowa

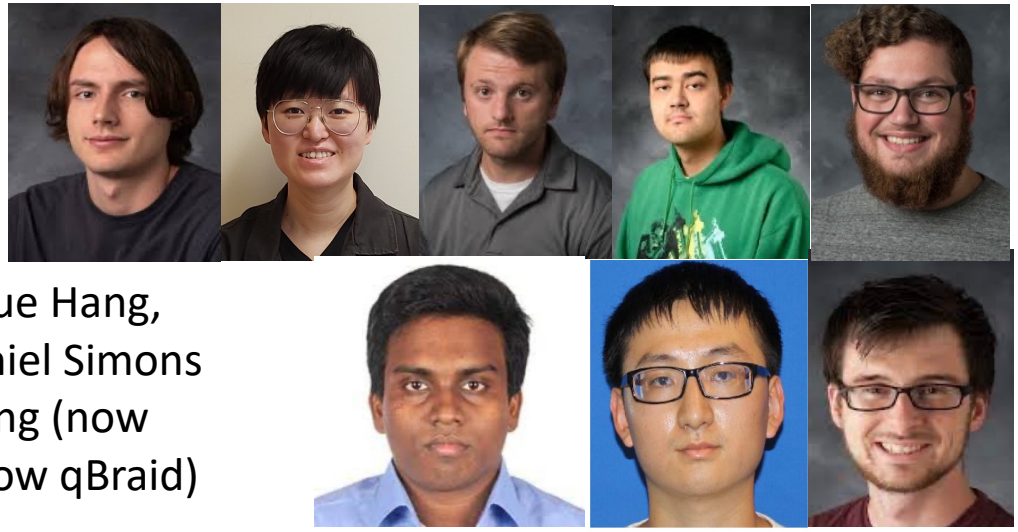

- Grad. students: James Corona, Zheyue Hang, Michael Hite, Robert Maxton, and Daniel Simons
- PostDocs: M. Asaduzzaman, Jin Zhang (now Chongqing U.) and Kenny Heitritter (now qBraid)

High-Energy Physics:

- B-meson decays with lattice gauge theory
- Composite models for the Higgs boson
- Applications of the Renormalization Group
- Tensor formulations of lattice field theory
- Machine learning in MC simulations

Quantum computing:

- Real-time evolution of field theory models
- Quantum computing (IBMQ and trapped ions)
- Quantum simulations (Rydberg atoms, QuEra)

Former graduate students

Yuzhi Liu (Ph. D. 2013): postdocs at U. Colorado Boulder and Indiana U.; Software engineer at Google
Haiyuan Zou (Ph. D. 2014): postdocs at Pittsburgh U. and T. D. Lee Center; Assistant Prof. at East China Normal Un.
J. Unmuth-Yockey (Ph. D. 2017): postdocs at Syracuse U. and Fermilab.
Z. Gelzer (Ph. D. 2017): postdoc at U. Illinois UC.
D. Floor (Ph. D. 2018), Software engineer in Brazil.
S. Foreman (Ph. D. 2019): postdoc at Argonne Nat. Lab.
E. Gustafson (Ph. D. 2021): postdoc at Fermilab
D. Simons (Ph. D. 2023)

QuLAT Collaboration

https://qulat.sites.uiowa.edu/

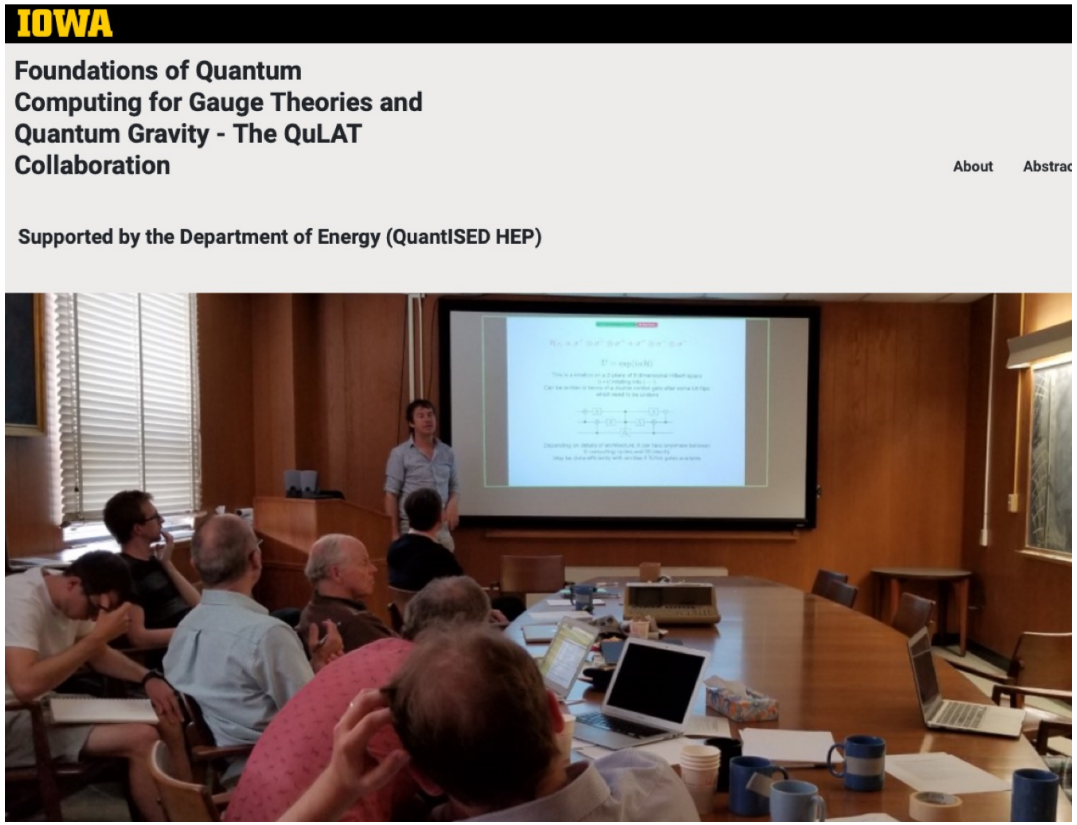

Goals of the collaboration

Quantum computers are expected to exceed the capacity of classical computers and to revolutionize several aspects of computation especially for the simulation of quantum systems. We develop new methods for using quantum computers to study aspects of the evolution of strongly interacting particles in collisions, the quantum behavior of gravitational systems and the emergence of space-time which are beyond the reach of classical computing. Our goal is to design the building blocks of universal quantum computers relevant for these problems and develop algorithms which scale reasonably with the size of the system.

Principal Investigators

Alexei Bazavov, Michigan State University
David Berenstein, University of Cal. Santa Barbara
Richard Brower, Boston University
Simon Catterall, Syracuse University
Xi Dong, UCSB (consultant)
Stephen Jordan, University of Maryland/Microsoft
Seth Lloyd, MIT (consultant)
Yannick Meurice, University of Iowa (Spokesperson)

Contents

Big picture

- Monte Carlo methods applied to Lattice Quantum Chromodynamics (QCD) at Euclidean time have been very successful at calculating the static properties of strongly interacting particles (masses, form factors, ...).
- These methods are not effective to deal with the real-time evolution of strongly interacting particles in collisions (jet physics, fragmentation, ...).
- Quantum computers or quantum simulation experiments offer new ways to deal with real time evolution.
- We need to start with simple models, use existing resources and build up towards Quantum Chromodynamics following the Euclidean time roadmap (the “Kogut sequence").
- We need to use actual Noisy Intermediate Scale Quantum (NISQ) machines and demonstrate progress for methods (economical truncations, large Trotter steps ...) and hardware.

Ab-initio jet physics : a realistic long term goal?

- Pythia, Herwig, and other jet simulation models encapsulate perturbative QCD results at short distance and empirical models to describe the large distance behavior.
- Crucial for the interpretation of collider physics experiments.
- Could we replace the large distance part by ab-initio lattice QCD calculations?

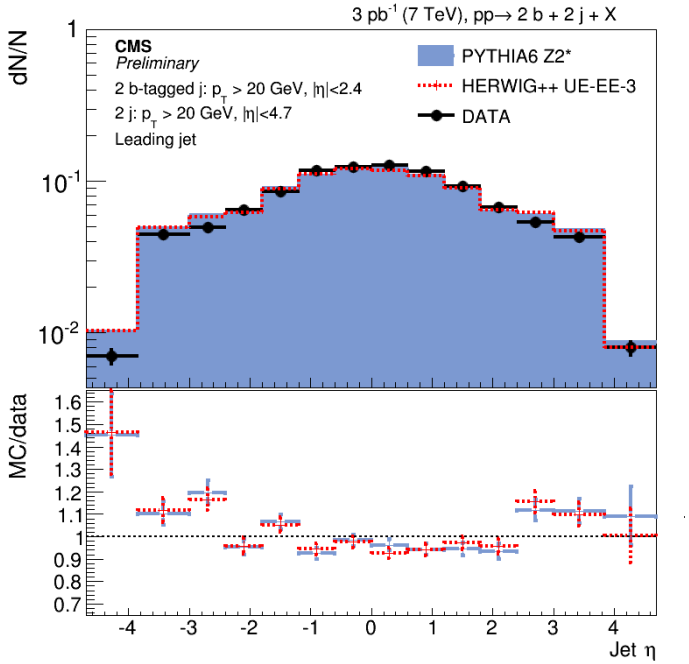

Figure: $pp \to b\bar{b}$ + jets, from CMS.

A first step: the quantum ising model in 1+1 dim.

Basic Trotter steps: PRD 99 09453

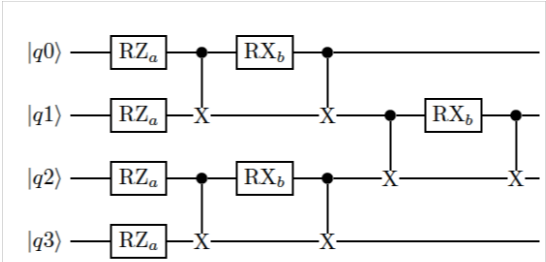

Figure 1: Circuit for 4 qubits with open boundary conditions

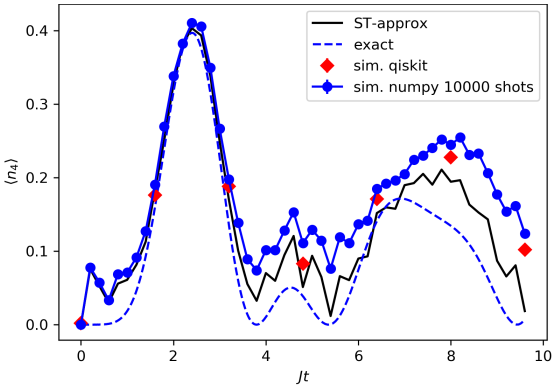

IBMQ Mitigations
JQST 6 045020

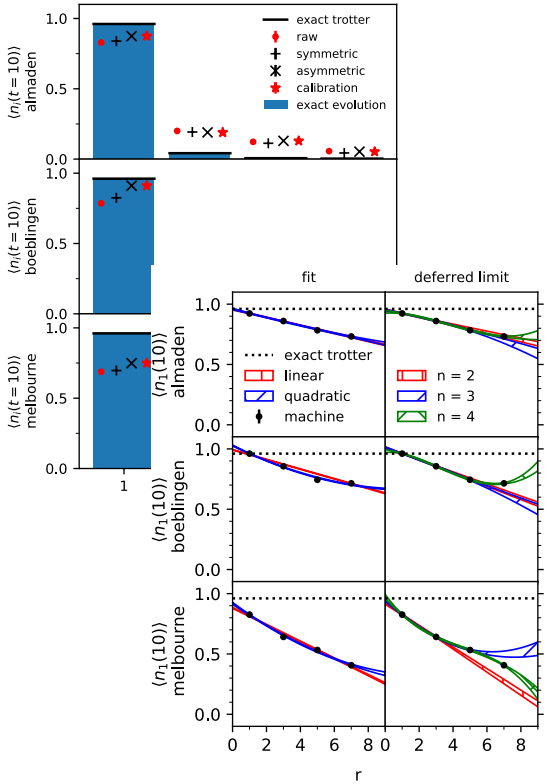

Phase shifts
PRD 104 054507

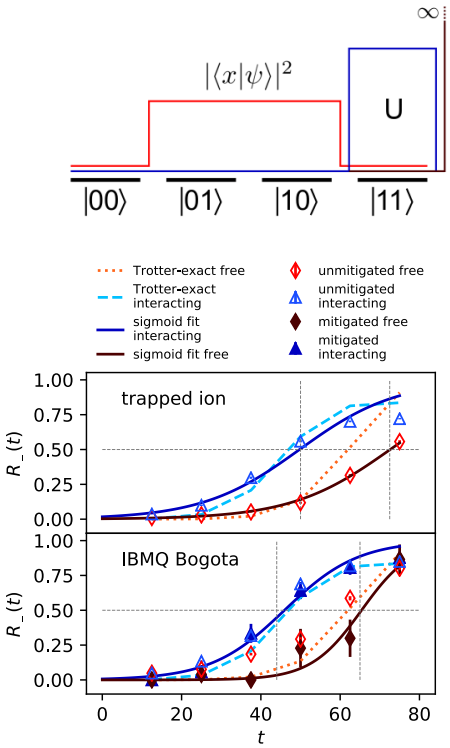

Discretization of problems classically intractable

Quantum computing (QC) requires a complete discretization

- Discretization of space: lattice gauge theory formulation
- Discretization of field integration: tensor methods

Important ideas of the tensor reformulation:

- Character expansions (such as Fourier series): partition function and averages become discrete sums of contracted tensors.
- The “hard" integrals are done exactly and field integrations provide Kronecker deltas that encode the symmetries.
- For continuous field variables, the sums are infinite, but truncations to finite sums do not break symmetries. Y. M., PRD 100, 014506 (2019) and PRD 102 014506 (2020).
- Tensors are the local building blocks of a new formulation

Refs: Y. M., R. Sakai, and J. Unmuth-Yockey, Tensor field theory with applications to quantum computing, arXiv:2010.06539; Reviews of Modern Physics Rev. Mod. Phys. 94, 025005.
Y. M., QFT: a quantum computation approach, IoP book.

Introductions to Tensor Field Theory

REVIEWS OF MODERN PHYSICS, VOLUME 94, APRIL–JUNE 2022

Tensor lattice field theory for renormalization and quantum computing

Yannick Meurice
Department of Physics and Astronomy, The University of Iowa, Iowa City, Iowa 52242, USA

Ryo Sakai
Department of Physics and Astronomy, The University of Iowa, Iowa City, Iowa 52242, USA and Department of Physics, Syracuse University, Syracuse, New York 13244, USA

Judah Unmuth-Yockey
Department of Physics, Syracuse University, Syracuse, New York 13244, USA and Fermi National Accelerator Laboratory, Batavia, Illinois 60510, USA

(published 26 May 2022)

The successes and limitations of statistical sampling for a sequence of models studied in the context of lattice QCD are discussed and the need for new methods to deal with finite-density and real-time evolution is emphasized. It is shown that these lattice models can be reformulated using tensorial methods where the field integrations in the path-integral formalism are replaced by discrete sums. These formulations involve various types of duality and provide exact coarse-graining formulas that can be combined with truncations to obtain practical implementations of the Wilson renormalization group program. Tensor reformulations are naturally discrete and provide manageable transfer matrices. Truncations with the time continuum limit are combined, and Hamiltonians suitable for performing quantum simulation experiments, for instance, using cold atoms, or to be programmed on existing quantum computers, are derived. Recent progress concerning the tensor field theory treatment of noncompact scalar models, supersymmetric models, economical four-dimensional algorithms, noise-robust enforcement of Gauss's law, symmetry preserving truncations, and topological considerations are reviewed. Connections with other tensor network approaches are also discussed.

DOI: 10.1103/RevModPhys.94.025005

CONTENTS

IOP Publishing | Bookstore

Home | Quantum Field Theory

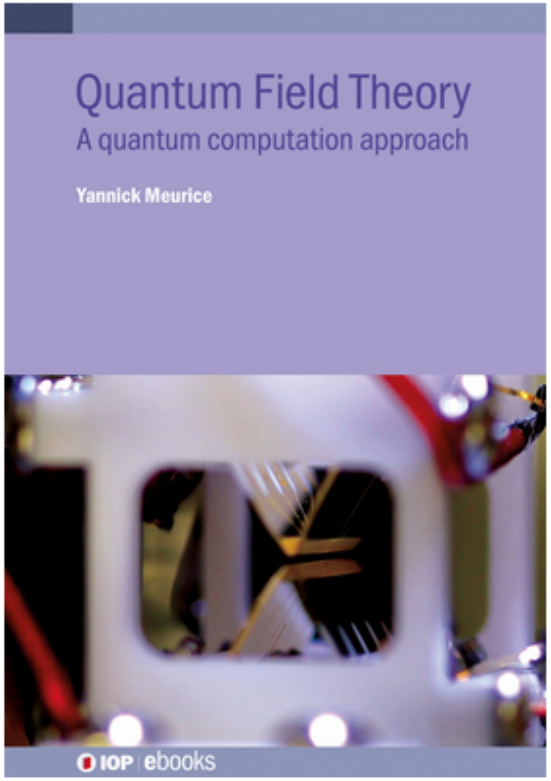

Interdisciplinary effort

INT WORKSHOP INT-21R-1C

Tensor Networks in Many Body and Quantum Field Theory

April 3, 2023 - April 7, 2023

ORGANIZERS

Simon Catterall
Syracuse University
smcatterall@gmail.com

Glen Evenbly
Georgia Institute of Technology
glen.evenbly@gmail.com

Yannick Meurice
University of Iowa
annick-meurice@uiowa.edu

Alessandro Roggero
University of Washington
roggero@uw.edu

DIVERSITY COORDINATOR

Alessandra Roggero
University of Washington
roggero@uw.edu

PROGRAM COORDINATOR

Paris Nguyen
Institute for Nuclear Theory
paris90@uw.edu

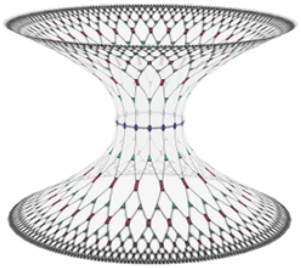

APPLICATION FORM - FOR FULL CONSIDERATION, APPLY BY NOVEMBER 27, 2022

OVERVIEW

Note to applicants: This is an in-person workshop. There is no virtual/online option for this event at this time. Please be aware that all participants must show proof of vaccination against COVID-19 upon arrival to the INT.

Disclaimer: Please also be aware that due to ongoing concerns regarding the COVID-19 pandemic, the workshop may be cancelled.

Tensor network methods are rapidly developing and evolving in many areas of quantum physics. They offer new ways of computing the properties of strongly interacting quantum matter. They provide new perspectives on theories with sign problems and/or significant entanglement. Tensor network ideas are also closely related to emerging efforts to design algorithms suitable for current and future quantum computing hardware or quantum simulation experiments. This workshop will bring together experts from a range of scientific fields with a common interest in these new methods

TLFT: From compact to discrete (O(2) example)

$$Z_{O(2)} = \prod_x \int_{-\pi}^{\pi} \frac{d\varphi_x}{2\pi} e^{\beta \sum_{x,\mu} \cos(\varphi_{x+\hat{\mu}} - \varphi_x)} = \mathrm{Tr} \prod_x T^{(x)}_{n_{x-\hat{1},1}, n_{x,1}, \ldots, n_{x,D}}.$$

$$e^{\beta \cos(\varphi_{x+\hat{\mu}} - \varphi_x)} = \sum_{n_{x,\mu}=-\infty}^{\infty} e^{i n_{x,\mu} \varphi_{x+\hat{\mu}}} I_{n_{x,\mu}}(\beta) e^{-i n_{x,\mu} \varphi_x}.$$

$$\text{Tensor}: \; T^{(x)}_{n_{x-\hat{1},1}, n_{x,1}, \ldots, n_{x-\hat{D},D}, n_{x,D}} = \sqrt{I_{n_{x-\hat{1},1}} I_{n_{x,1}}, \ldots, I_{n_{x-\hat{D},D}} I_{n_{x,D}}} \times \delta_{n_{x,\mathrm{out}}, n_{x,\mathrm{in}}},$$

$$\prod_x \int_{-\pi}^{\pi} d\varphi_x \Longrightarrow \sum_{\{n\}}$$

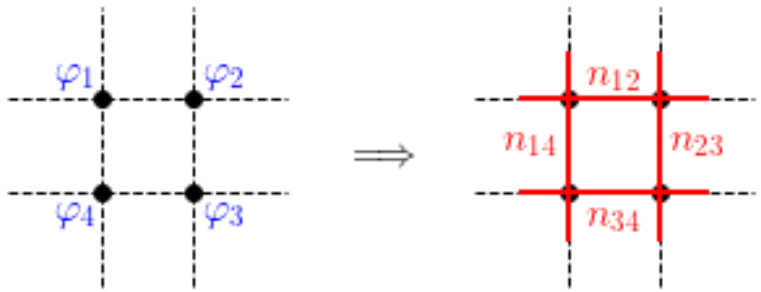

The gauged version is the Abelian Higgs model.

Coarse-graining/point-splitting

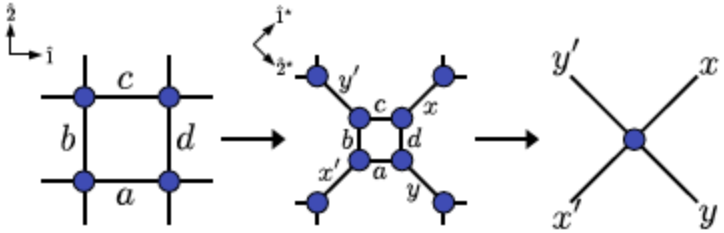

FIG. 13. A coarse-graining step for the tensor network. Circles represent tensors and closed indices should be contracted. The definitions of the unit vectors for the original and the coarse-grained network are also shown. The tensor indices are shown in the same manner as in Eq. (94).

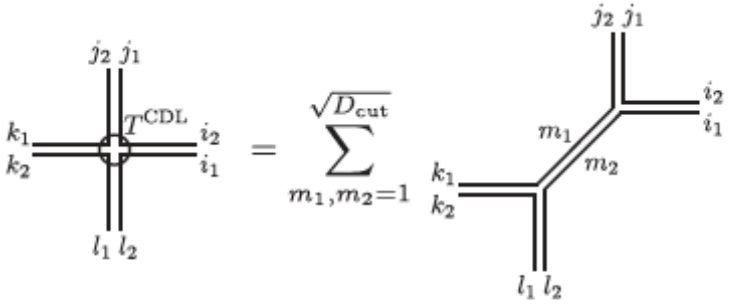

FIG. 21. SVD of a CDL tensor.

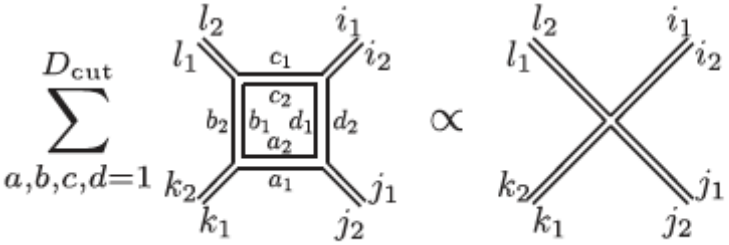

Compact Abelian Higgs Model (CAHM)

The lattice compact Abelian Higgs model is a non-perturbative regularized formulation of scalar quantum electrodynamics (scalar electrons-positrons + photons with compact fields).

$$Z_{CAHM} = \prod_x \int_{-\pi}^{\pi} \frac{d\varphi_x}{2\pi} \prod_{x,\mu} \int_{-\pi}^{\pi} \frac{dA_{x,\mu}}{2\pi} e^{-S_{gauge}-S_{matter}},$$

$$S_{gauge} = \beta_{plaquette} \sum_{x,\mu<\nu} (1 - \cos(A_{x,\mu} + A_{x+\hat{\mu},\nu} - A_{x+\hat{\nu},\mu} - A_{x,\nu})),$$

$$S_{matter} = \beta_{link} \sum_{x,\mu} (1 - \cos(\varphi_{x+\hat{\mu}} - \varphi_x + A_{x,\mu})).$$

- local invariance: $\varphi'_x = \varphi_x + \alpha_x$ and $A'_{x,\mu} = A_{x,\mu} - (\alpha_{x+\hat{\mu}} - \alpha_x)$.
- φ is the Nambu-Goldstone mode of the original model. The Brout-Englert-Higgs mode is decoupled (heavy).

Assembly of the A (links, blue) and B (plaquette, red) tensors for $D = 2$ (Figures by Ryo Sakai)

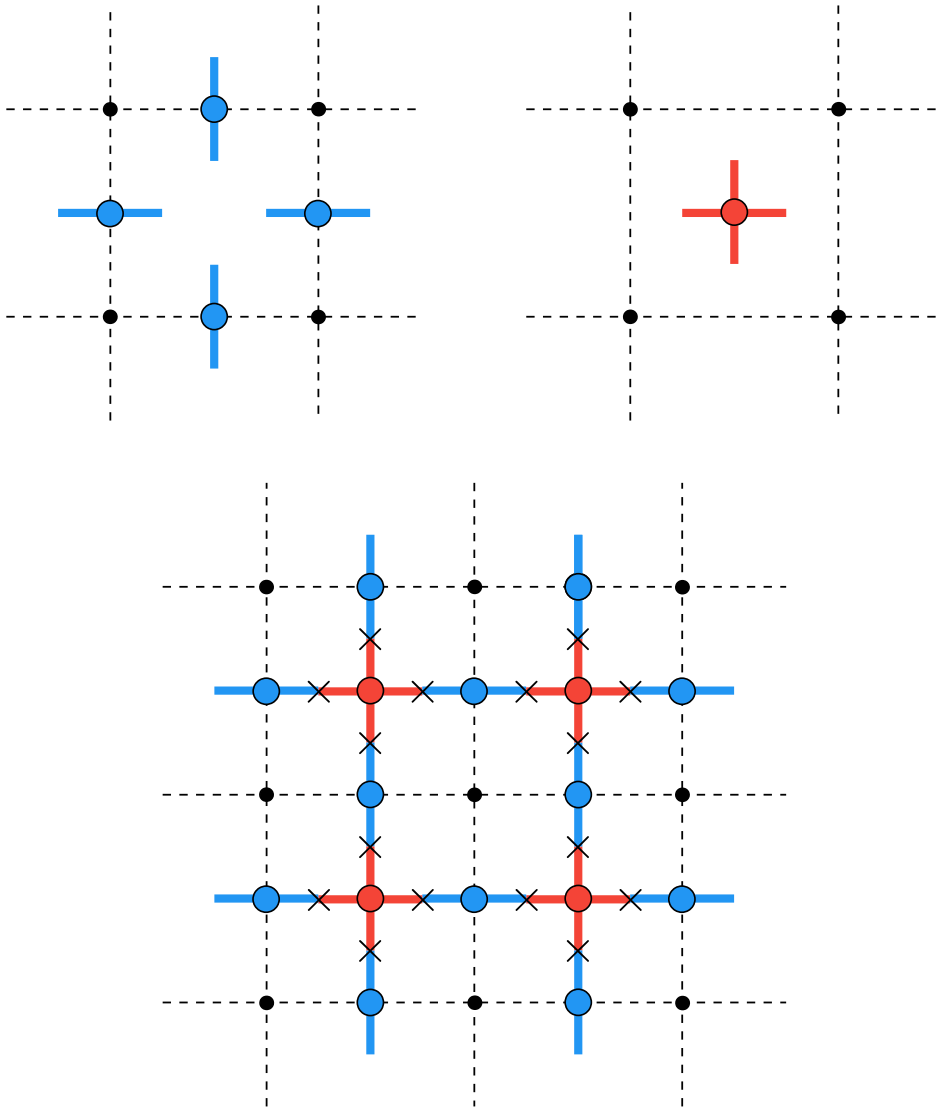

Assembly of the A (links, blue) and B (plaquette, red) tensors for $D = 3$ (Figures by Ryo Sakai)

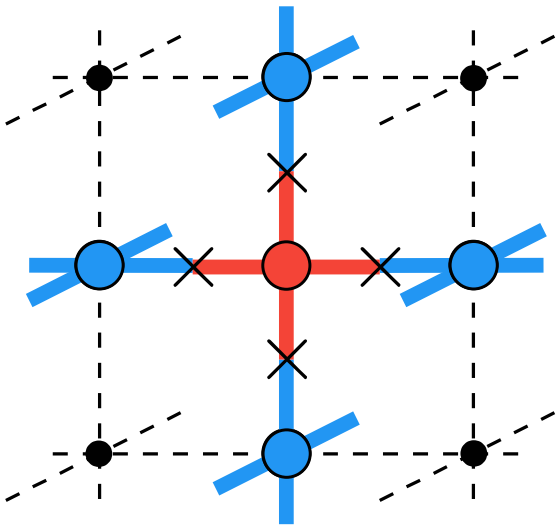

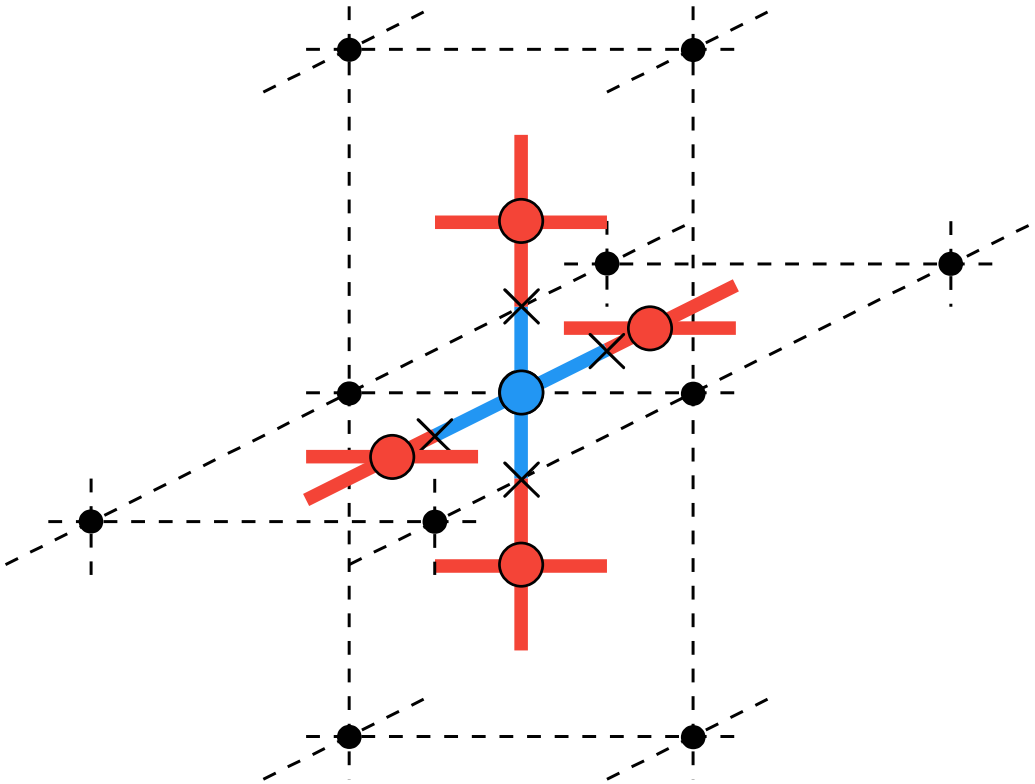

Transfer matrix and Gauss's law with NISQ machines

PHYSICAL REVIEW D **102,** 014506 (2020)

Discrete aspects of continuous symmetries in the tensorial formulation of Abelian gauge theories

Yannick Meurice*

Department of Physics and Astronomy, The University of Iowa, 514 Van Allen Hall, Iowa City, Iowa 52242, USA

(Received 7 April 2020; accepted 30 June 2020; published 14 July 2020)

We show that standard identities and theorems for lattice models with $U(1)$ symmetry get reexpressed discretely in the tensorial formulation of these models. We also explain the geometrical analogy between the continuous lattice equations of motion and the discrete selection rules of the tensors. We further construct a gauge-invariant transfer matrix in arbitrary dimensions, show the equivalence with its gauge-fixed version in a maximal temporal gauge, and explain how a discrete Gauss's law is always enforced. Moreover, we propose a noise-robust way to implement Gauss's law in arbitrary dimensions, and we reformulate Noether's theorem for global, local, continuous, or discrete Abelian symmetries: for each given symmetry, there is one corresponding tensor redundancy. We discuss semiclassical approximations for classical solutions with periodic boundary conditions in two solvable cases, and we show the correspondence of their weak coupling limit with the tensor formulation after Poisson summation. Finally, we briefly discuss connections with other approaches and implications for quantum computing.

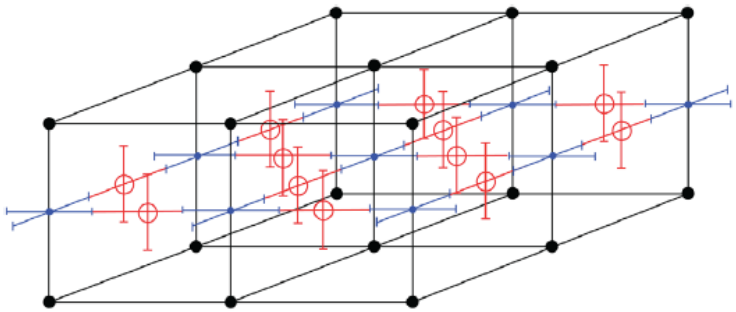

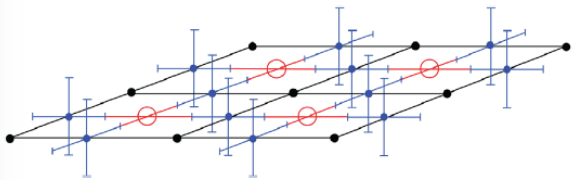

FIG. 3. Magnetic layer of the transfer matrix for $D = 3$ on a time slice. Small circles (blue) are used for the A tensors and large circles (red) for the B tensors.

FAQ: Do truncations break global symmetries? No (Y.M. arXiv 1903.01918, PRD 100, 014506)

- Truncations of the tensorial sums are necessary, but do they break the symmetries of the model?
- Non-linear O(2) sigma model and its gauged version (the compact Abelian Higgs model), on a D-dimensional cubic lattice: truncations are compatible with symmetry identities.
- This selection rule is due to the quantum number selection rules at the sites and is independent of the particular values taken by the tensors (e. g. 0, discrete form of a vector calculus theorem).
- Extends to global $O(3)$ symmetries (you need to keep all the m's for a given ℓ, related to Wigner-Eckart)
- The universal properties of these models can be reproduced with highly simplified formulations desirable for implementations with quantum computers or for quantum simulations experiments.

AHM: Hamiltonian and Hilbert space in 1+1 dim.

The continuous-time limit yields the Hamiltonian

$$H = \frac{U}{2}\sum_{i=1}^{N_s}(L_i^z)^2 + \frac{Y}{2}\sum_i (L_{i+1}^z - L_i^z)^2 - X\sum_{i=1}^{N_s} U_i^x$$

with $U^x \equiv \frac{1}{2}(U^+ + U^-)$ and $L^z|m\rangle = m|m\rangle$ and $U^\pm|m\rangle = |m \pm 1\rangle$.

- m is a discrete electric field quantum number ($-\infty < m < +\infty$)
- In practice, we need to apply truncations: $U^\pm|\pm m_{max}\rangle = 0$.
- We focus on the spin-1 truncation ($m = \pm 1, 0$ and $U^x = L^x/\sqrt{2}$.)
- U-term: electric field energy.
- Y-term: matter charges (determined by Gauss's law)
- X-term: currents inducing temporal changes in the electric field.

Target simulations (E-field, spin-1, 5 sites)

$$H = \frac{U}{2}\sum_{i=1}^{N_s}\left(L_i^z\right)^2 + \frac{Y}{2}\sum_i (L_{i+1}^z - L_i^z)^2 - X\sum_{i=1}^{N_s} U_i^x$$

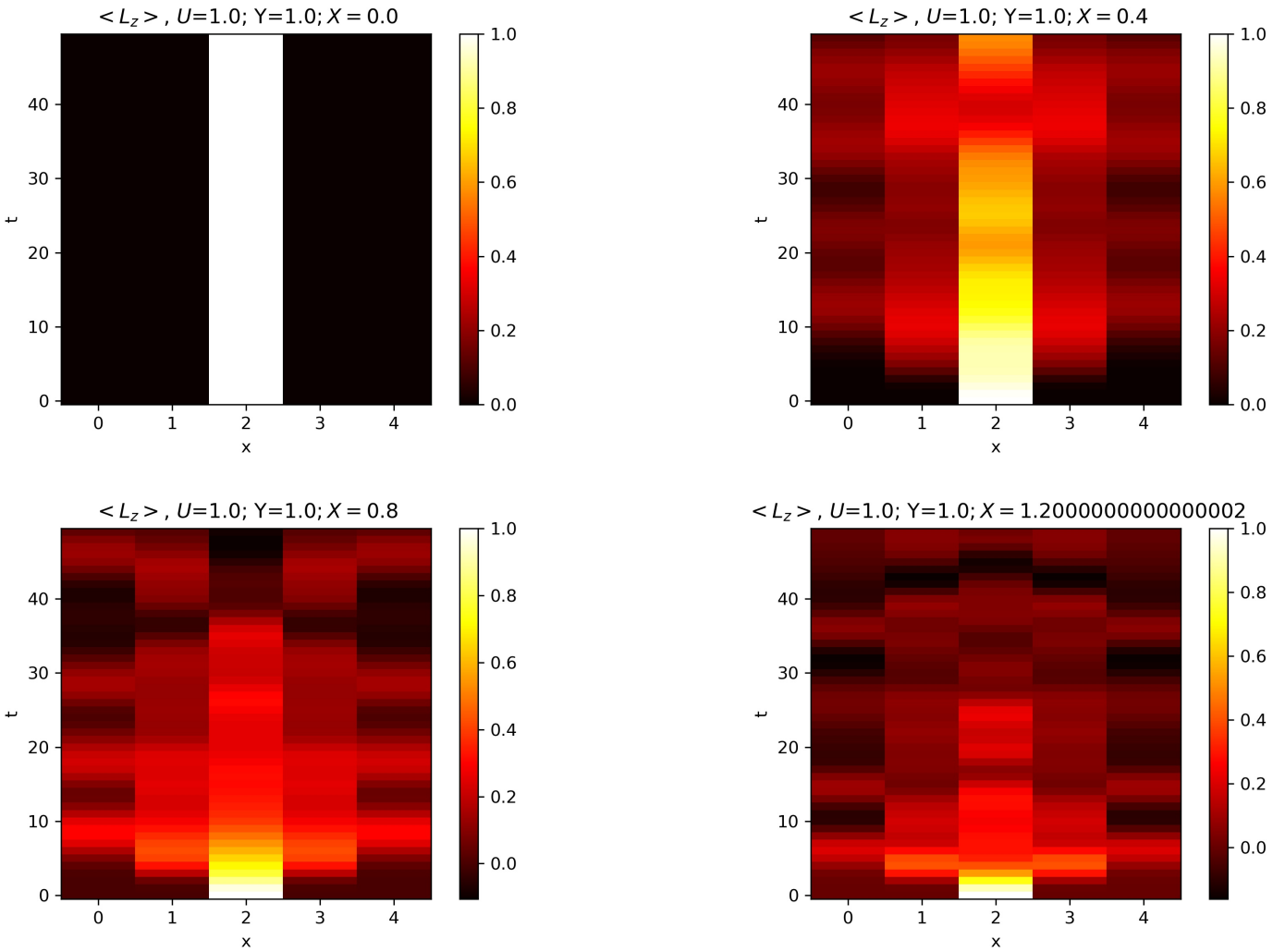

Target (E-field, spin-1, 5 sites, various limits)

$$H = \frac{U}{2}\sum_{i=1}^{N_s}\left(L_i^z\right)^2 + \frac{Y}{2}\sum_i (L_{i+1}^z - L_i^z)^2 - X\sum_{i=1}^{N_s} U_i^x$$

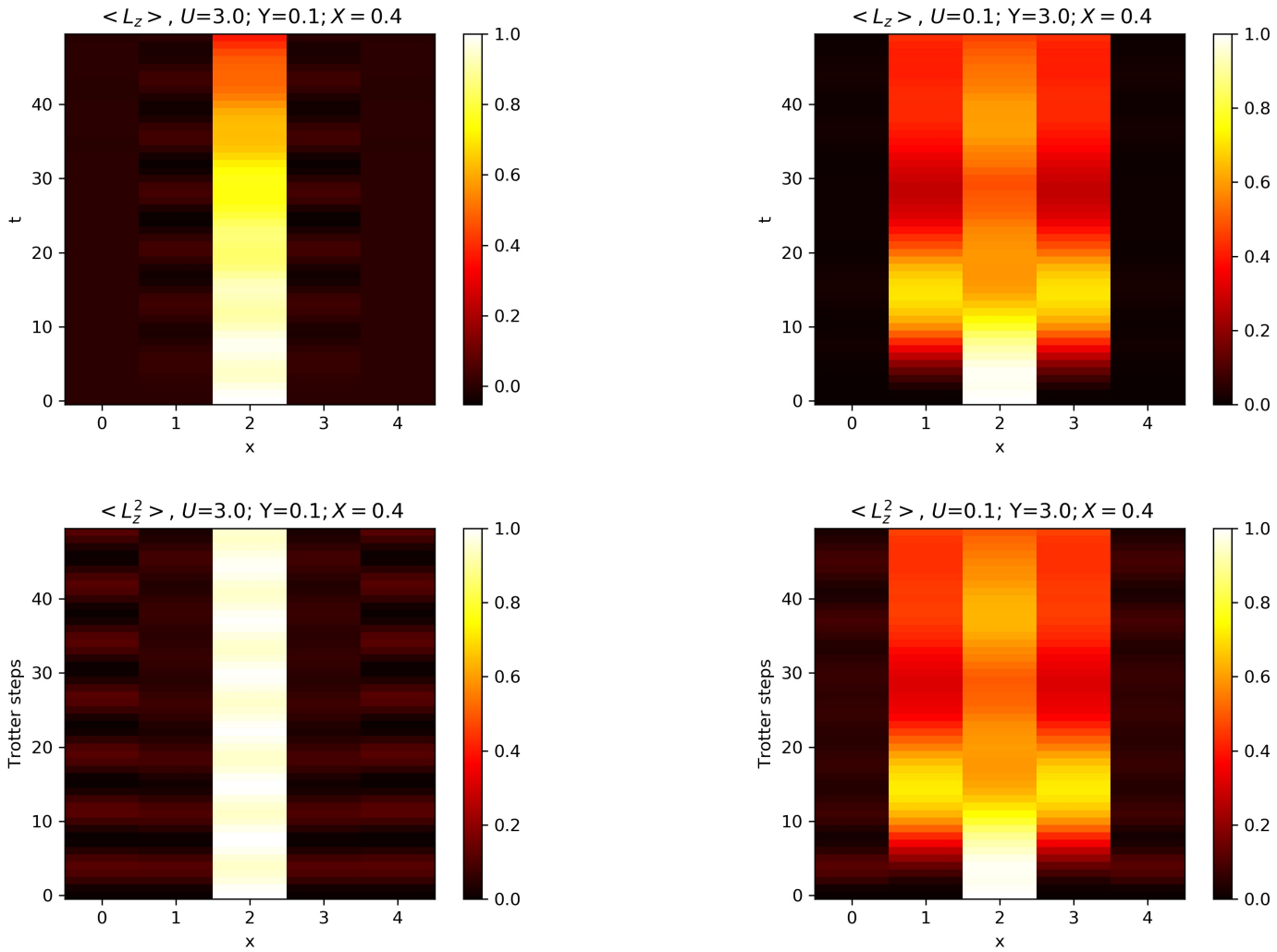

Target (E-field, spin-1, 5 sites, other examples)

$$H = \frac{U}{2}\sum_{i=1}^{N_s}\left(L_i^z\right)^2 + \frac{Y}{2}\sum_i (L_{i+1}^z - L_i^z)^2 - X\sum_{i=1}^{N_s} U_i^x$$

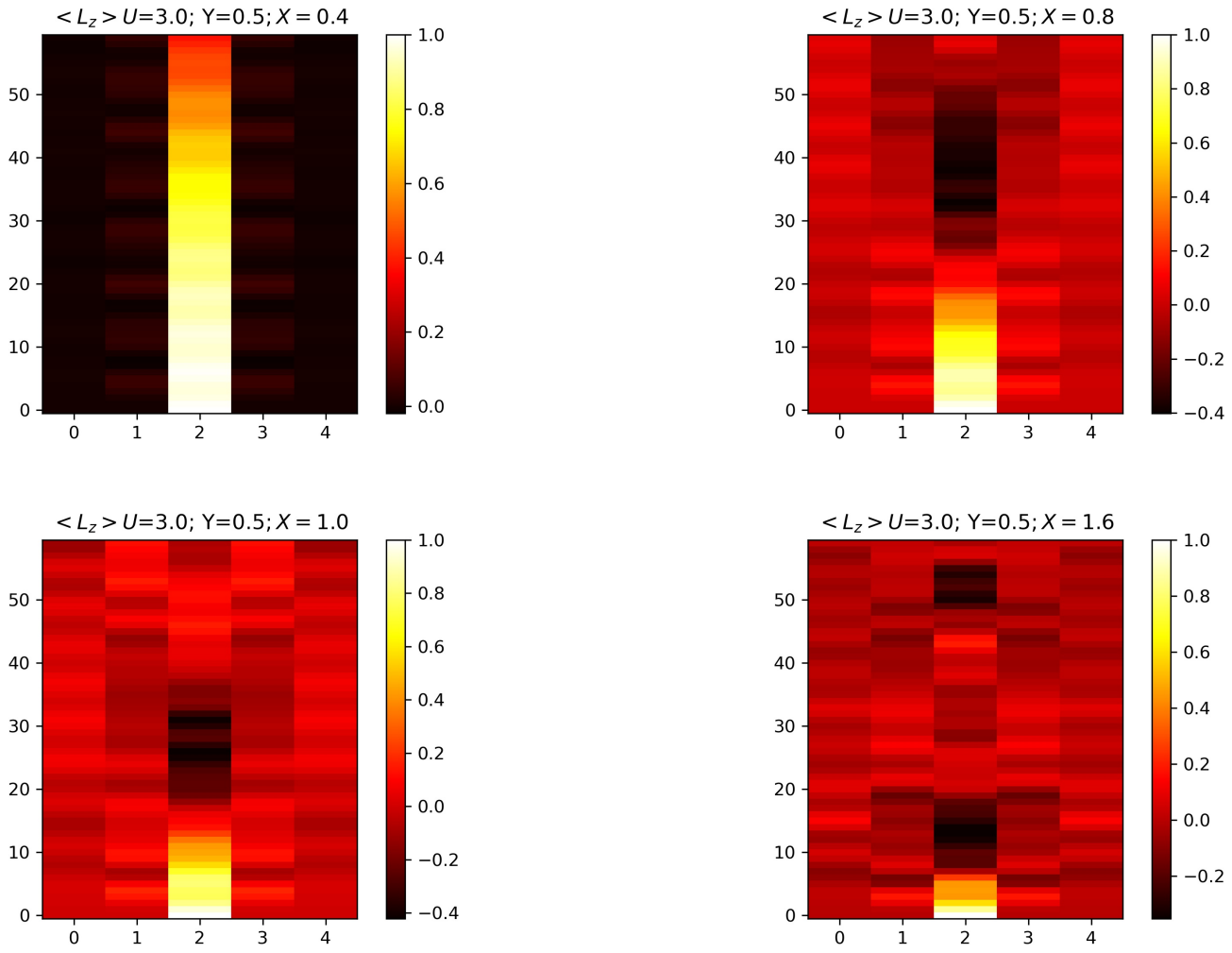

Stark localization

```
nmax = 10;
hh = ConstantArray[0, {nmax, nmax}];
gg = .1; hl = 0.5;
Do[hh[[nn, nn + 1]] = gg; hh[[nn + 1, nn]] = gg, {nn, 1, nmax - 1}];
Do[hh[[nn, nn]] = hl * nn, {nn, 1, nmax}];

MatrixForm[hh]
```

$$\begin{pmatrix} 0.5 & 0.1 & 0 & 0 & 0 & 0 & 0 & 0 & 0 & 0 \\ 0.1 & 1. & 0.1 & 0 & 0 & 0 & 0 & 0 & 0 & 0 \\ 0 & 0.1 & 1.5 & 0.1 & 0 & 0 & 0 & 0 & 0 & 0 \\ 0 & 0 & 0.1 & 2. & 0.1 & 0 & 0 & 0 & 0 & 0 \\ 0 & 0 & 0 & 0.1 & 2.5 & 0.1 & 0 & 0 & 0 & 0 \\ 0 & 0 & 0 & 0 & 0.1 & 3. & 0.1 & 0 & 0 & 0 \\ 0 & 0 & 0 & 0 & 0 & 0.1 & 3.5 & 0.1 & 0 & 0 \\ 0 & 0 & 0 & 0 & 0 & 0 & 0.1 & 4. & 0.1 & 0 \\ 0 & 0 & 0 & 0 & 0 & 0 & 0 & 0.1 & 4.5 & 0.1 \\ 0 & 0 & 0 & 0 & 0 & 0 & 0 & 0 & 0.1 & 5. \end{pmatrix}$$

```
Eigenvalues[hh]
```

{5.01962, 4.50038, 4., 3.5, 3., 2.5, 2., 1.5, 0.99962, 0.480382}

```
eig = Eigenvectors[hh];
Do[Print[ListPlot[Table[{mm, eig[[nn, mm]]}, {mm, 1, nmax}], Joined → True,
   PlotRange → All]], {nn, 1, nmax}]
```

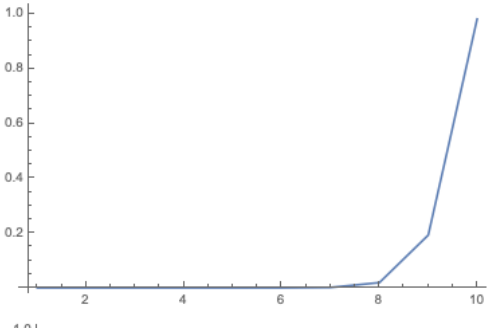

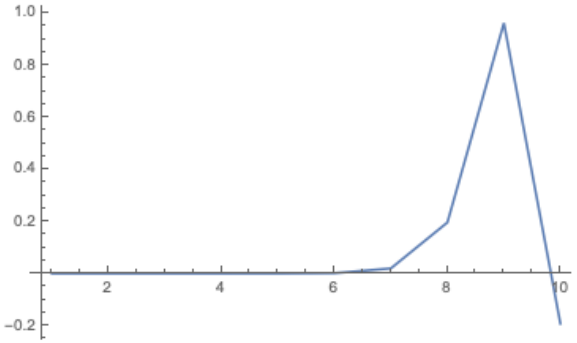

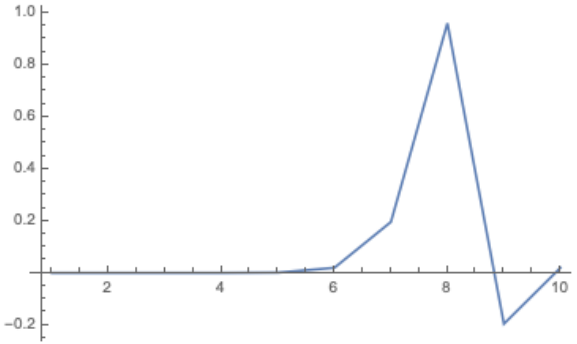

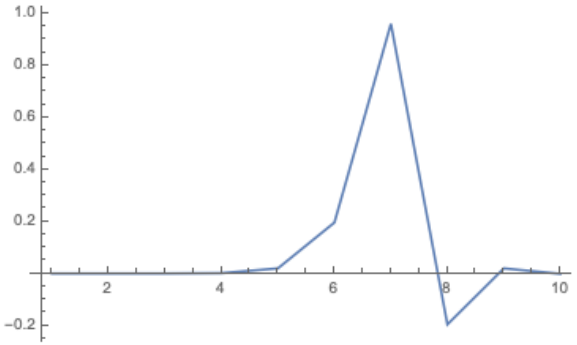

Nearest neighbor Rydberg-dressed interactions

PHYSICAL REVIEW LETTERS **121,** 223201 (2018)

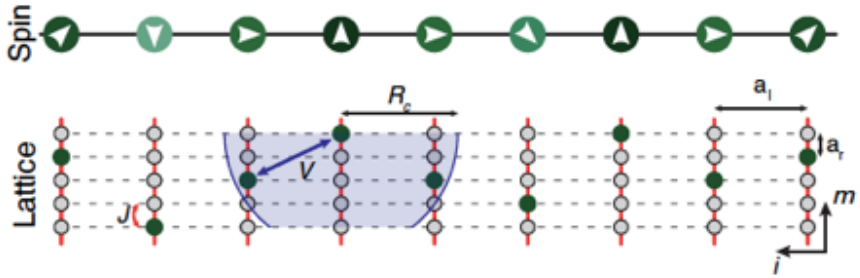

FIG. 3. Multileg ladder implementation for spin-2. The upper part shows the possible m_z projections. Below, we show the corresponding realization in a ladder within an optical lattice. The atoms (green disks) are allowed to hop within a rung with a strength J, while no hopping is allowed along the legs. The lattice constants along rungs and legs are a_r and a_l, respectively. Coupling between atoms in different rungs is implemented via an isotropic Rydberg-dressed interaction V with a cutoff distance R_c (marked by blue shading).

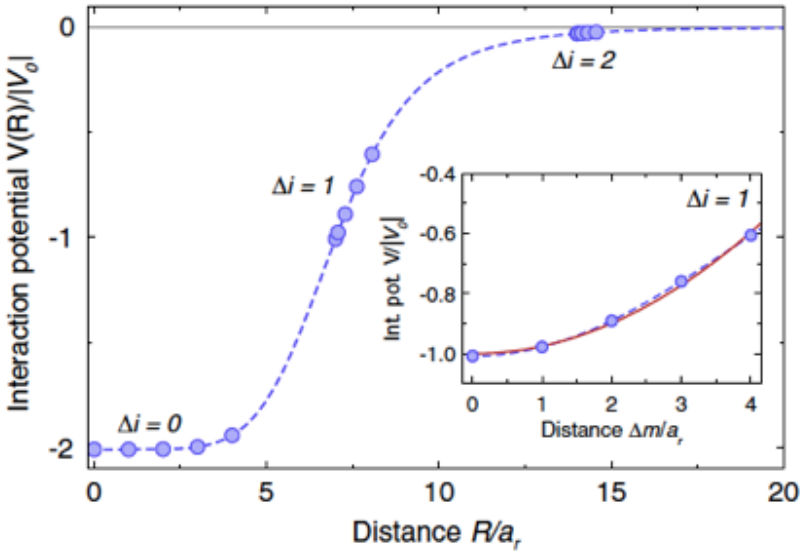

FIG. 4. Quadratic interactions on an asymmetric ladder for $s = 2$. The isotropic Rydberg-dressed potential (dashed blue line)

Quantum Simulation of the Universal Features of the Polyakov Loop

Jin Zhang,[1] J. Unmuth-Yockey,[2] J. Zeiher,[3] A. Bazavov,[4] S.-W. Tsai,[1] and Y. Meurice[5]

Proposal to quantum simulate the 1+1 Abelian Higgs model using a ladder of Rydberg atoms. The horizontal dimension is space, the vertical direction is the electric field degree of freedom.

Optical lattice proposal (with J. Zeiher, MPQ)

Earlier spin-2 proposal on an optical lattice with Rydberg dressed atoms (PRL 121 223201); vertical dimension is the spin

$$H = \frac{U}{2}\sum_i \left(L^z_{(i)}\right)^2 + \frac{Y}{2}\sum_i (L^z_{(i)} - L^z_{(i+1)})^2 - X\sum_i U^x_{(i)}$$

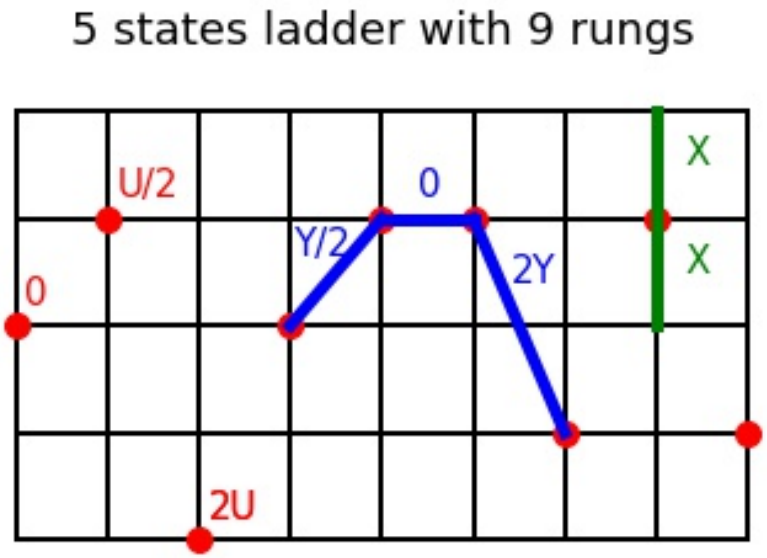

Figure: Ladder with one atom per rung: tunneling along the vertical direction only ($L^z = \pm 2,\ \pm 1,\ 0$, green), short range attractive interactions (blue). A parabolic potential is applied in the spin (vertical) direction (red).

Configurable Arrays of Rydberg Atoms (CARA)

LETTER

https://doi.org/10.1038/s41586-019-1070-1

Quantum Kibble–Zurek mechanism and critical dynamics on a programmable Rydberg simulator

Alexander Keesling[1], Ahmed Omran[1], Harry Levine[1], Hannes Bernien[1], Hannes Pichler[1,2], Soonwon Choi[1], Rhine Samajdar[1], Sylvain Schwartz[3], Pietro Silvi[4,5], Subir Sachdev[1], Peter Zoller[4,5], Manuel Endres[6], Markus Greiner[1], Vladan Vuletić[7] & Mikhail D. Lukin[1]*

Quantum phase transitions (QPTs) involve transformations between different states of matter that are driven by quantum fluctuations[1]. These fluctuations play a dominant part in the quantum critical region surrounding the transition point, where the dynamics is governed by the universal properties associated with the QPT. Although time-dependent phenomena associated with classical, thermally driven phase transitions have been extensively studied in systems ranging from the early Universe to Bose–Einstein condensates[2–5], understanding critical real-time dynamics in isolated, non-equilibrium quantum systems remains a challenge[6]. Here we use a Rydberg atom quantum simulator with

We investigate quantum criticality using a reconfigurable one-dimensional array of ^{87}Rb atoms with programmable interactions[21]. In our system, 51 atoms in the electronic ground state $|g\rangle$, which are evenly separated by a controllable distance, are homogeneously coupled to the excited Rydberg state $|r\rangle$, in which they experience van der Waals interactions with a strength that decays as $V(r) \propto 1/r^6$, where r is the interatomic distance. This system is described by the many-body Hamiltonian,

$$\frac{\mathcal{H}}{\hbar} = \frac{\Omega}{2}\sum_i (|g_i\rangle\langle r_i| + |r_i\rangle\langle g_i|) - \Delta\sum_i n_i + \sum_{i<j} V_{ij} n_i n_j \qquad (1)$$

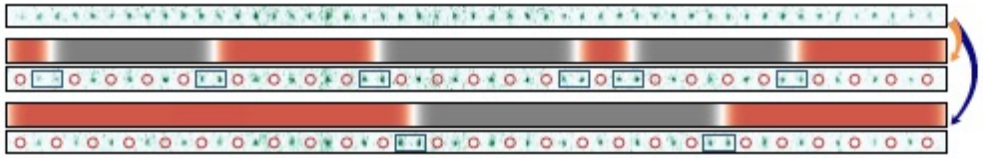

Fig. 2 | QKZM for a QPT into the $\mathbb{Z}_2$-ordered phase. a, Single-shot images of the atom array before and after a fast (orange arrow) and a slow (blue arrow) sweep across the phase transition, showing larger average sizes of correlated domains for the slower sweep. Green spots (open circles) represent atoms in $|g\rangle$ ($|r\rangle$). Blue rectangles mark the position of domain walls, and the red and grey coloured regions highlight the extent of the correlated domains. **b**, Correlation length growth and saturation as

208 | NATURE | VOL 568 | 11 APRIL 2019

Configurable Arrays of Rydberg Atoms (CARA)

PHYSICAL REVIEW D **104,** 094513 (2021)

Theoretical methods to design and test quantum simulators for the compact Abelian Higgs model

Yannick Meurice

Department of Physics and Astronomy, The University of Iowa, Iowa City, Iowa 52242 USA

(Received 30 July 2021; accepted 4 October 2021; published 22 November 2021)

The lattice compact Abelian Higgs model is a nonperturbative regularized formulation of low-energy scalar quantum electrodynamics. In $1+1$ dimensions, this model can be quantum simulated using a ladder-shaped optical lattice with Rydberg-dressed atoms [J. Zhang*et al.*, Phys. Rev. Lett. **121**, 223201 (2018)]. In this setup, one spatial dimension is used to carry the angular momentum of the quantum rotors. One can use truncations corresponding to spin-2 and spin-1 to build local Hilbert spaces associated with the links of the lattice. We argue that ladder-shaped configurable arrays of Rydberg atoms can be used for the same purpose. We make concrete proposals involving two and three Rydberg atoms to build one local spin-1 space (a qutrit). We show that the building blocks of the Hamiltonian calculations are models with one and two spins. We compare target and simulators using perturbative and numerical methods. The two-atom setup provides an easily controllable simulator of the one-spin model while the three-atom setup involves solving nonlinear equations. We discuss approximate methods to couple two spin-1 spaces. The article provides analytical and numerical tools necessary to design and build the proposed simulators with current technology.

DOI: 10.1103/PhysRevD.104.094513

CARA simulators

- One can adapt the optical lattice construction to configurable arrays of Rydberg atoms denoted CARA.
- They can be configured by positioning ^{87}Rb atoms separated by controllable (but not too small) distances, homogeneously coupled to the excited Rydberg state $|r\rangle$ with a detuning Δ.
- The ground state is denoted $|g\rangle$ and the two possible states $|g\rangle$ and $|r\rangle$ can be seen as a qubit. $n|g\rangle = 0,\ n|r\rangle = |r\rangle$.
- The Hamiltonian reads

$$H = \frac{\Omega}{2}\sum_i (|g_i\rangle\langle r_i| + |r_i\rangle\langle g_i|) - \Delta \sum_i n_i + \sum_{i<j} V_{ij} n_i n_j,$$

with

$$V_{ij} = \Omega R_b^6 / r_{ij}^6,$$

for a distance r_{ij} between the atoms labelled as i and j.
- This repulsive interaction prevents two atoms close enough to each other to be both in the $|r\rangle$ state. This is the so-called blockade mechanism.

One site spin-1 with 2 and 3 atoms (PRD 104)

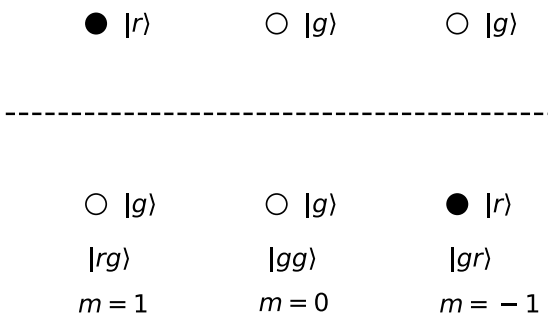

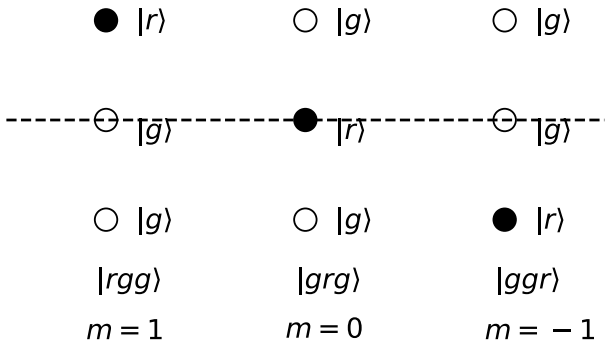

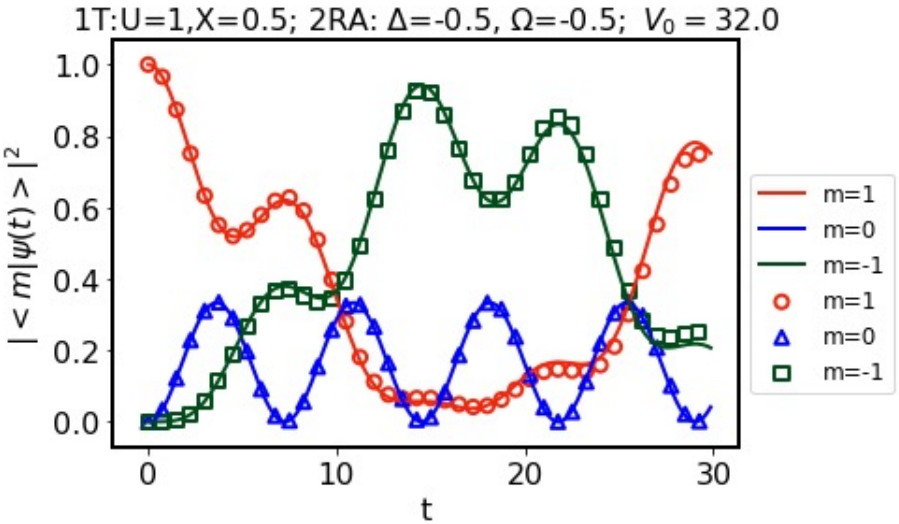

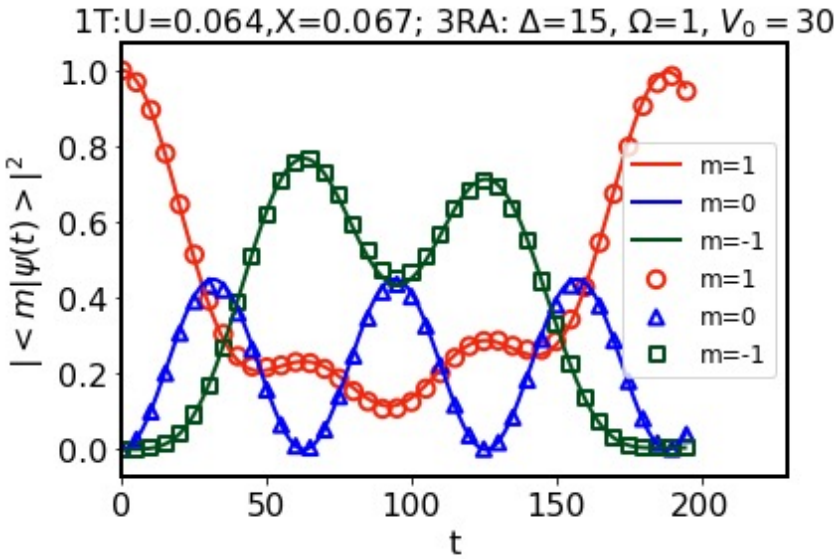

Solid line: target, Symbols: simulator

Two sites with 4 and 6 atoms (PRD 104)

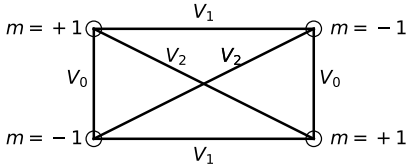

$$\rho \equiv \frac{a_r}{a_s},$$

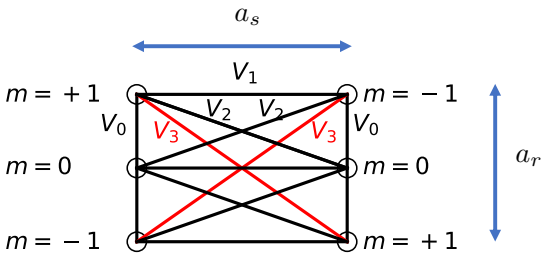

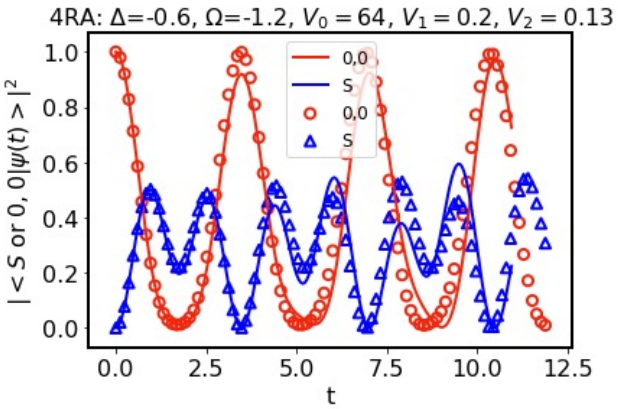

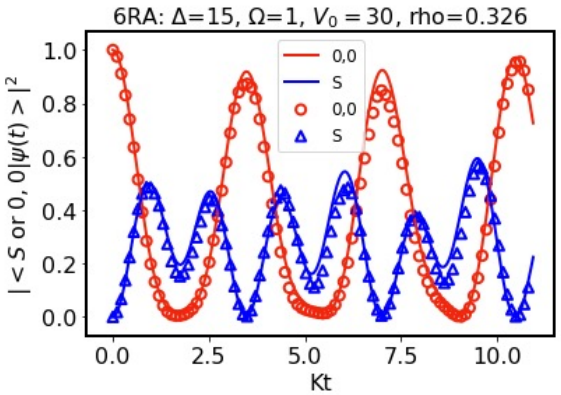

$$|S>\equiv \frac{1}{2}(|0,1>+|0,-1>+|1,0>+|-1,0>).$$

Solid line: target, Symbols: simulator. Note: precise matching is not crucial, what is important is the continuum limit. Rich critical behavior .

Exact matching vs. study of continuum limit

- 1 site, 2 atoms: exact up to $|rr\rangle$ transitions (when $\Omega = 0$, can be implemented by setting $\Delta = -U/2$ and $\Omega = -X$
- 2 sites, 4 atoms: when $X = \Omega = 0$ reads $\Delta = -U/2 - \frac{Y}{2},\ V_1 = Y,\ V_2 = -Y$. No solution with current technology (homogeneous setup).
- 1 site, 3 atoms: it's complicated! (ideally: inhomogeneous Δ to split $m = 0$ and $m = \pm 1$, otherwise use degenerate perturbation theory as a guide, James Corona's work in progress).

A better approach may be to study all the continuum limits (where correlation lengths become large) that can be obtained with the simulator.

Experimental implementation in progress

Experimental Plans:

Check the real-time evolutions for 2, 3, 4 and 6 atoms with realistic choices of parameters:
Rabi frequency $\Omega \sim 2\pi$ MHz
Detuning $|\Delta| < 2\pi$ 20 MHz
Lattice spacing: dx, $dy > 3\mu$m
Total run time $T < 4\mu$s

Explore the critical behavior of long ladders using arrays with hundreds of atoms

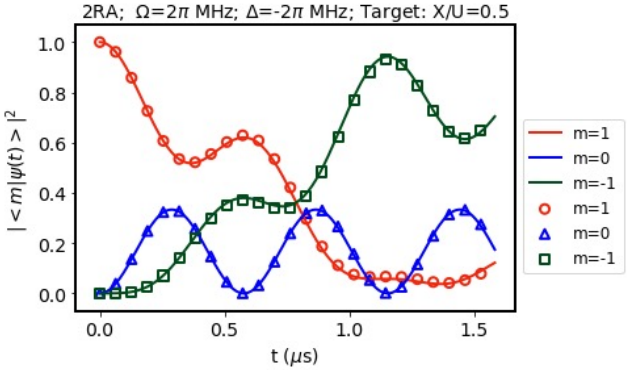

QuEra projects

Quasi-independent pairs with strong Rydberg blockade

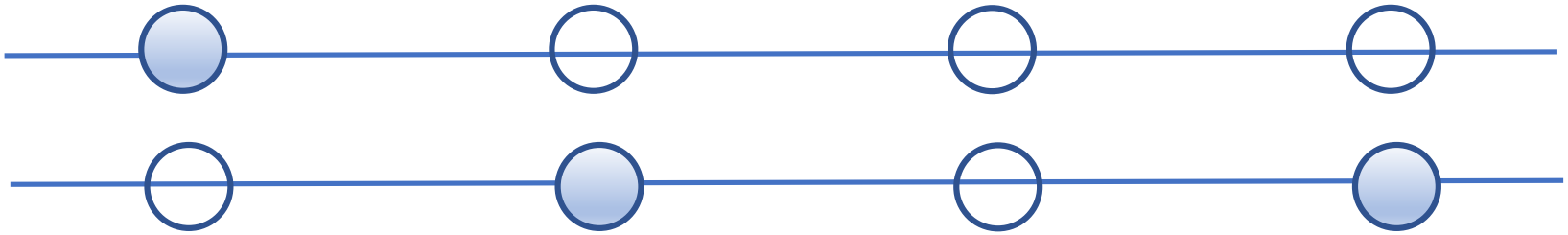

Interacting ladders

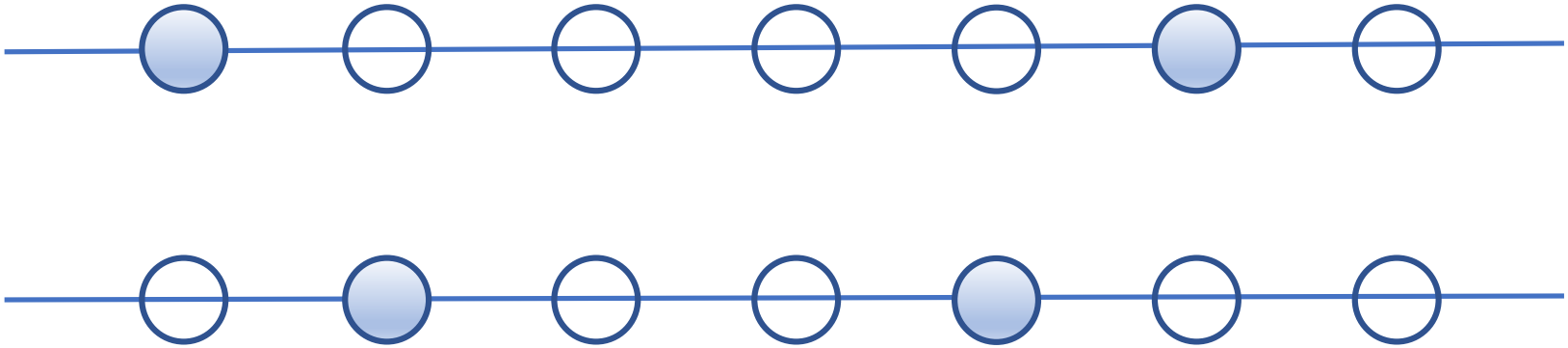

QuEra projects

2 – Legged Rydberg Ladder (Average Image)

Rb = 8.7 um.

Rb/a = 1
N atoms = 44 (22x2)

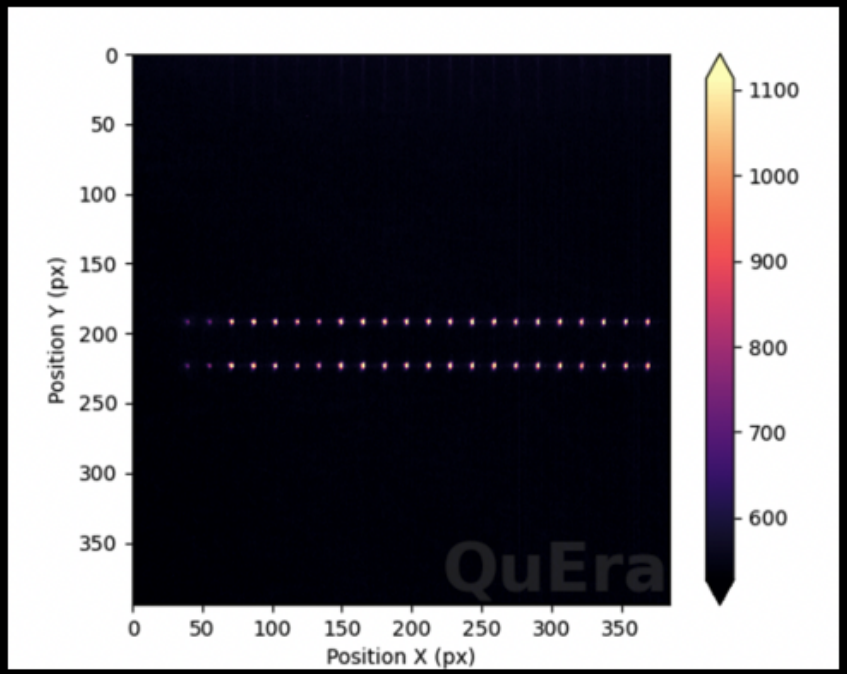

Rb/a = 3,
N atoms = 126 (68x2)

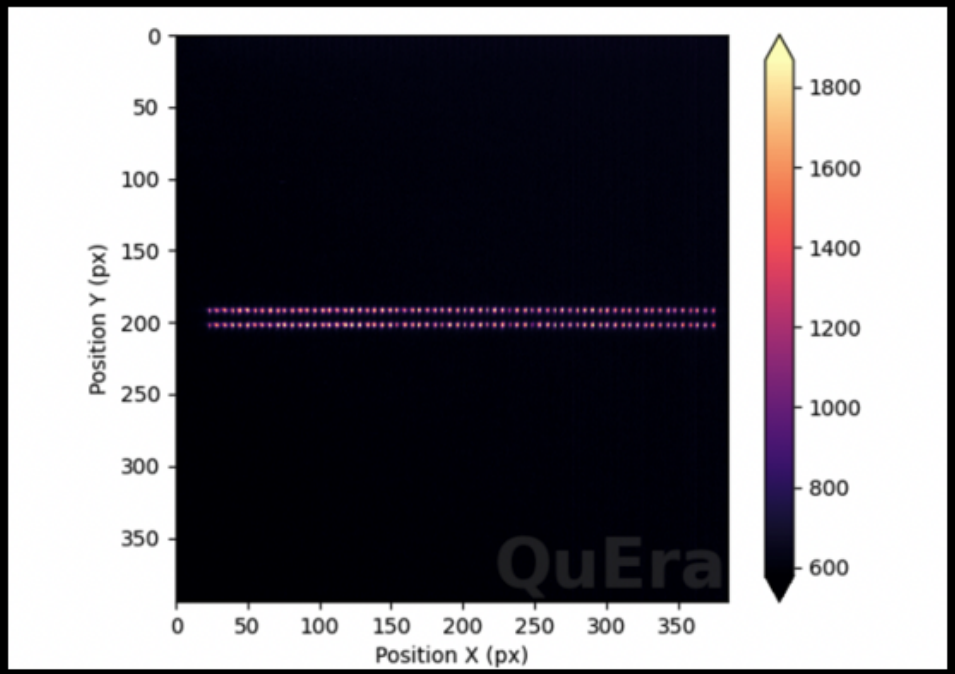

QuEra- Aquila

Easy access to quantum hardware

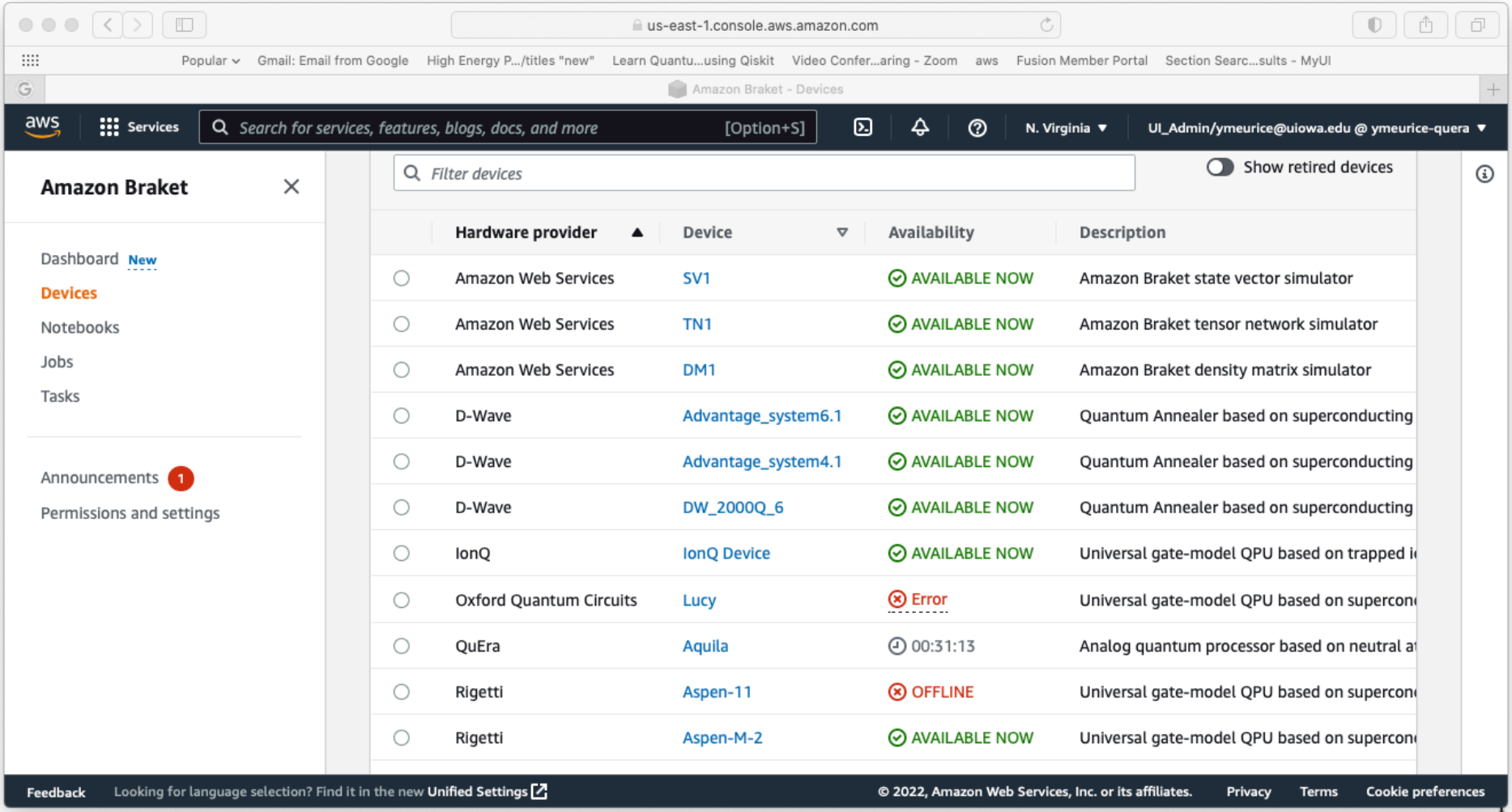

Easy access to quantum hardware

awstest/amazon-braket-exampl | myanalog - Jupyter Notebook

localhost:8888/notebooks/awstest/amazon-braket-examples/examples/analog_hamiltonian_simulation/myan 80%

Getting Started | Legal | Slack | 2101.09220.pdf | Pomona Pitzer | Other Bookmarks

jupyter myanalog Last Checkpoint: 11 hours ago (autosaved) | Logout

File Edit View Insert Cell Kernel Widgets Help | Not Trusted | Python 3

Run | Markdown

```
register.add([0, 0])
register.add([a, 0.0])
register.add([2*a, 0.0])
register.add([0.0,a])
register.add([a, a])
register.add([2*a, a]);
```

The atom arrangement can be visualized in the following way

In [10]:

```
from utils import show_register

show_register(register)
```

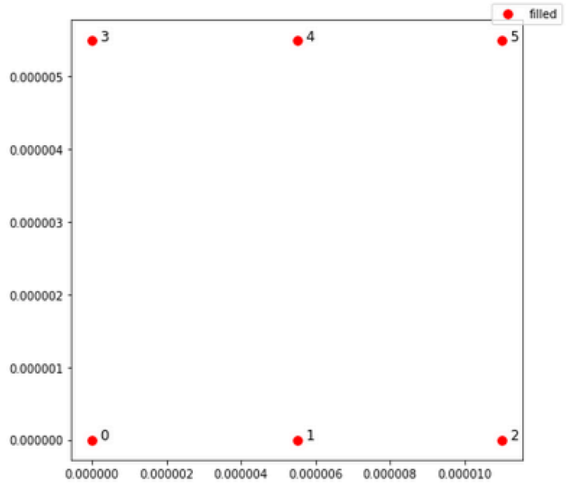

Driving field

The first term of the Hamiltonian represents the effect of a **driving field** that addresses the atoms simultaneously and uniformly

Easy access to quantum hardware

localhost:8888/notebooks/awstest/amazon-braket-examples/examples/analog_hamilto

jupyter myanalog Last Checkpoint: Last Monday at 9:27 PM (autosaved)

We can run the AHS program just like running a quantum circuit on other Braket devices

In [7]:
```
result = device.run(ahs_program, shots=1000).result()
```

To confirm that we indeed arrive at a maximally entangled state, we first collect the measurement results, followed by counting the number of occurence of $|gr\rangle$ and $|rg\rangle$ respectively.

In [8]:
```
def get_counters_from_result(result):
    post_sequences = [list(measurement.post_sequence) for measurement in result.measurements]
    post_sequences = ["".join(['r' if site==0 else 'g' for site in post_sequence]) for post_sequence in post_sec

    counters = {}
    for post_sequence in post_sequences:
        if post_sequence in counters:
            counters[post_sequence] += 1
        else:
            counters[post_sequence] = 1
    return counters

get_counters_from_result(result)
```

Out[8]:
```
{'gggggg': 306,
 'gggggr': 28,
 'ggggrg': 79,
 'gggrgg': 27,
 'gggrgr': 82,
 'ggrggg': 39,
 'ggrrgg': 134,
 'grgggg': 86,
 'rggggg': 25,
 'rggggr': 117,
 'rgrggg': 77}
```

The simulation outcome indeed confirms our expectations

1. It is very unlikely to excite the 3rd atom to the Rydberg state because of the strong local detuning.
2. Due to the Rydberg blockade, it is very unlikely to excite the 1st and 2nd atoms to the Rydberg states simultaneously
3. By appropriately tuning the Rabi frequency and the duration of the AHS program, we can arrive at a maximally entangled state for the 1st and 2nd atoms. Since our simulation is noiseless, the discrepancy from ideal 50%-50% split is attributed to statistical sampling (aka "shot noise").

Aquila run (Kenny Heitritter)

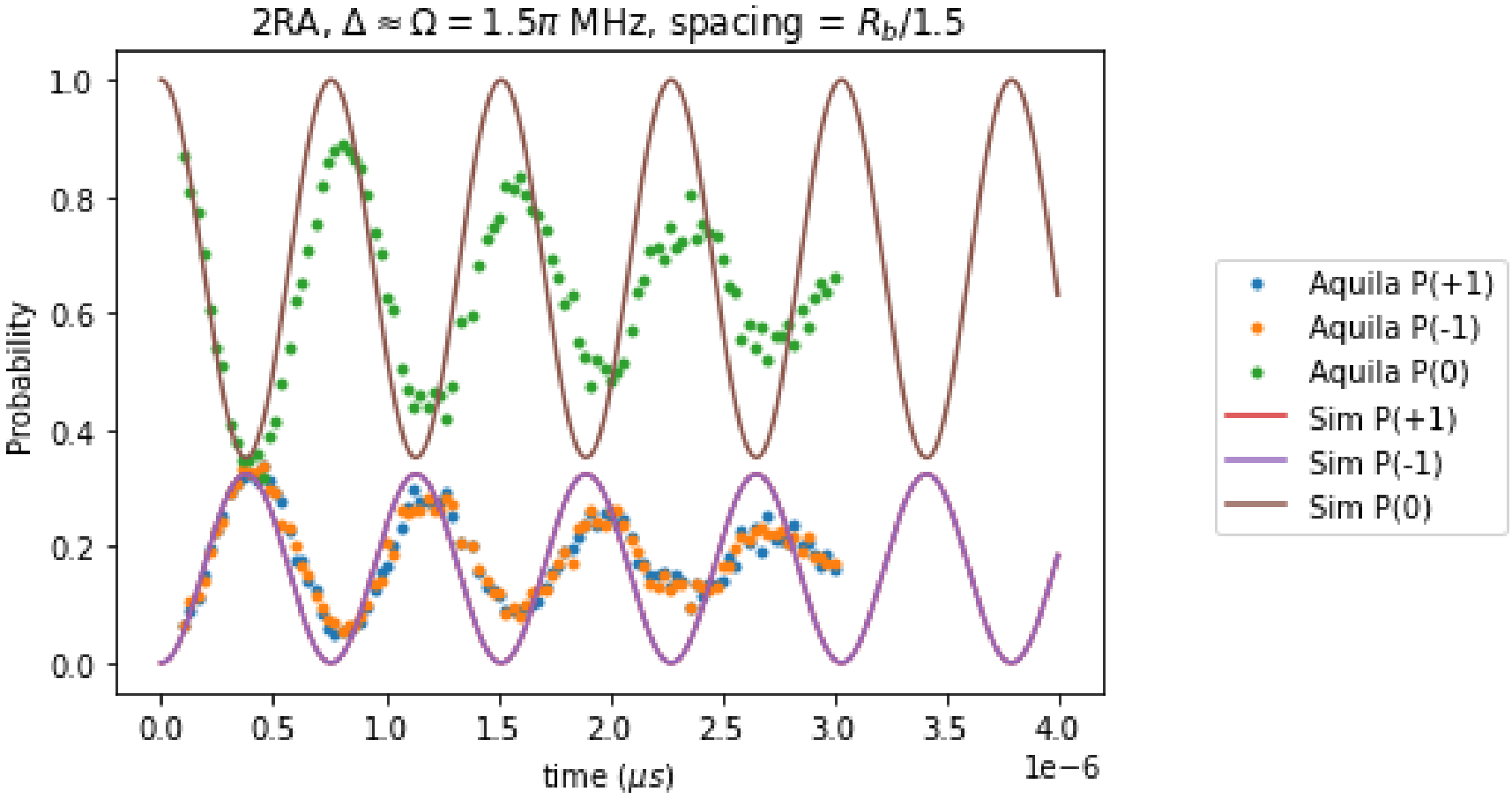

Fragmentation with a two-leg ladder (Kenny Heitritter)

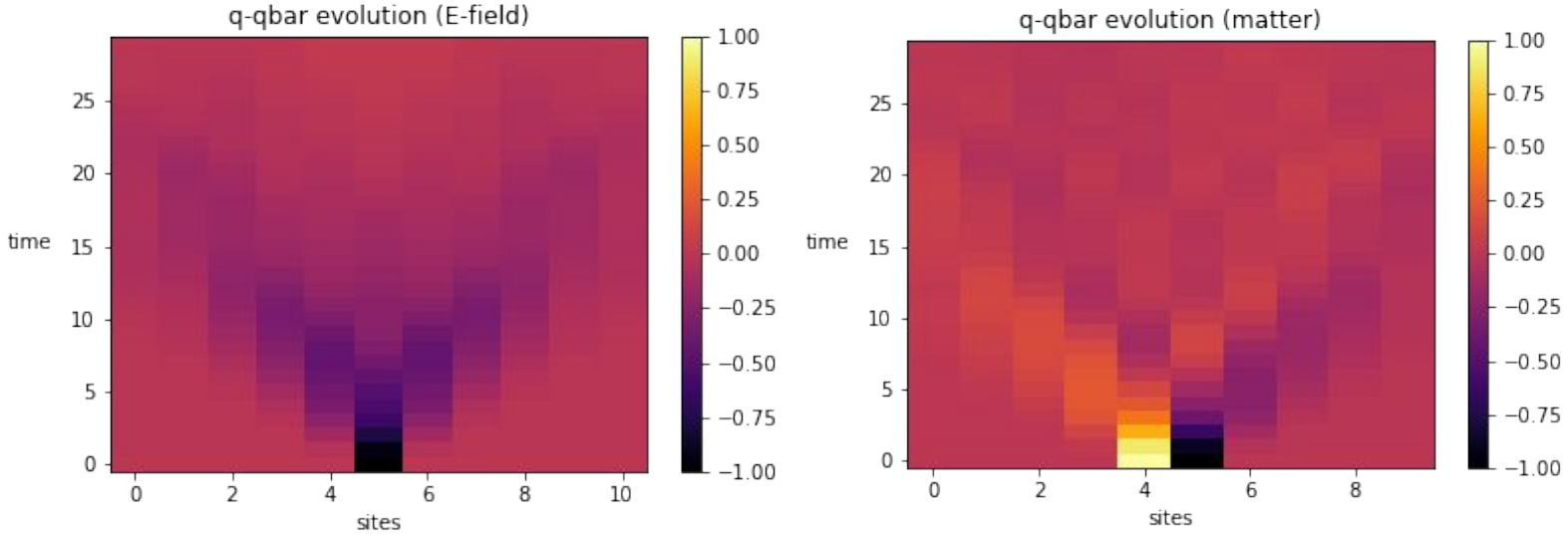

E-fields: Bright is S=+1, Dark is S=-1, Pink=0
Matter: Bright is quark, Dark is antiquark, Pink is vacuum
22 atoms; $\Delta/\Omega = 2.2$, $R_b/a = 2$, $dy = 2dx$.

CARA phase diagrams

Probing many-body dynamics on a 51-atom quantum simulator (single chain) Hannes Bernien, Sylvain Schwartz, Alexander Keesling, Misha Lukin et al. (Nature 511). Ladder phase diagram under study (Jin Zhang, S.-W. Tsai et al.)

ARTICLE RESEARCH

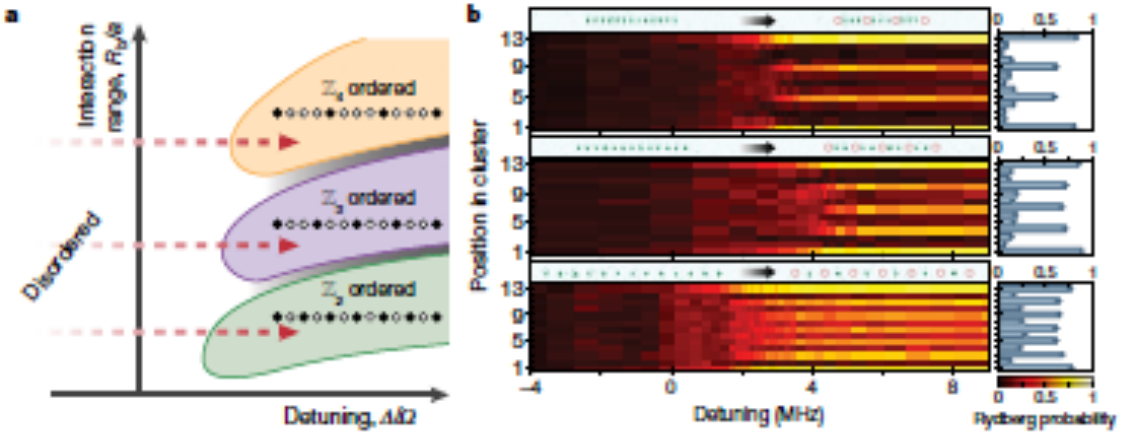

Figure 2 | Phase diagram and build-up of crystalline phases. a, A schematic of the ground-state phase diagram of the Hamiltonian in equation (1) displays phases with various broken symmetries depending on the interaction range R_b/a (R_b, blockade radius; a, trap spacing) and detuning Δ (see main text). Shaded areas indicate potential incommensurate phases[30]. Here we show the experimentally accessible region; further details can be found in refs 30, 33 and 36. **b,** The build-up of Rydberg crystals on a 13-atom array is observed by slowly changing the laser parameters, as indicated by the red dashed arrows in **a** (see also Fig. 3a). The bottom panel shows a configuration in which the atoms are $a = 5.74\,\mu$m apart, which results in a nearest-neighbour interaction of $V_{i,i+1} = 2\pi \times 24$ MHz and leads to $\mathbb{Z}_2$ order whereby every other atom is excited to the Rydberg state $|r\rangle$. The bar plot on the right displays the final, position-dependent Rydberg probability (error bars denote 68% confidence intervals). The configuration in the middle panel ($a = 3.57\,\mu$m, $V_{i,i+1} = 2\pi \times 414.3$ MHz) results in $\mathbb{Z}_3$ order and the top panel ($a = 2.87\,\mu$m, $V_{i,i+1} = 2\pi \times 1{,}536$ MHz) in $\mathbb{Z}_4$ order. For each configuration, we show a single-shot fluorescence image before (left) and after (right) the pulse. Red circles highlight missing atoms, which are attributed to Rydberg excitations.

Phase diagram for a two-leg ladder (Jin Zhang)

4.2 Two-leg ladder: $dx = dy/2$

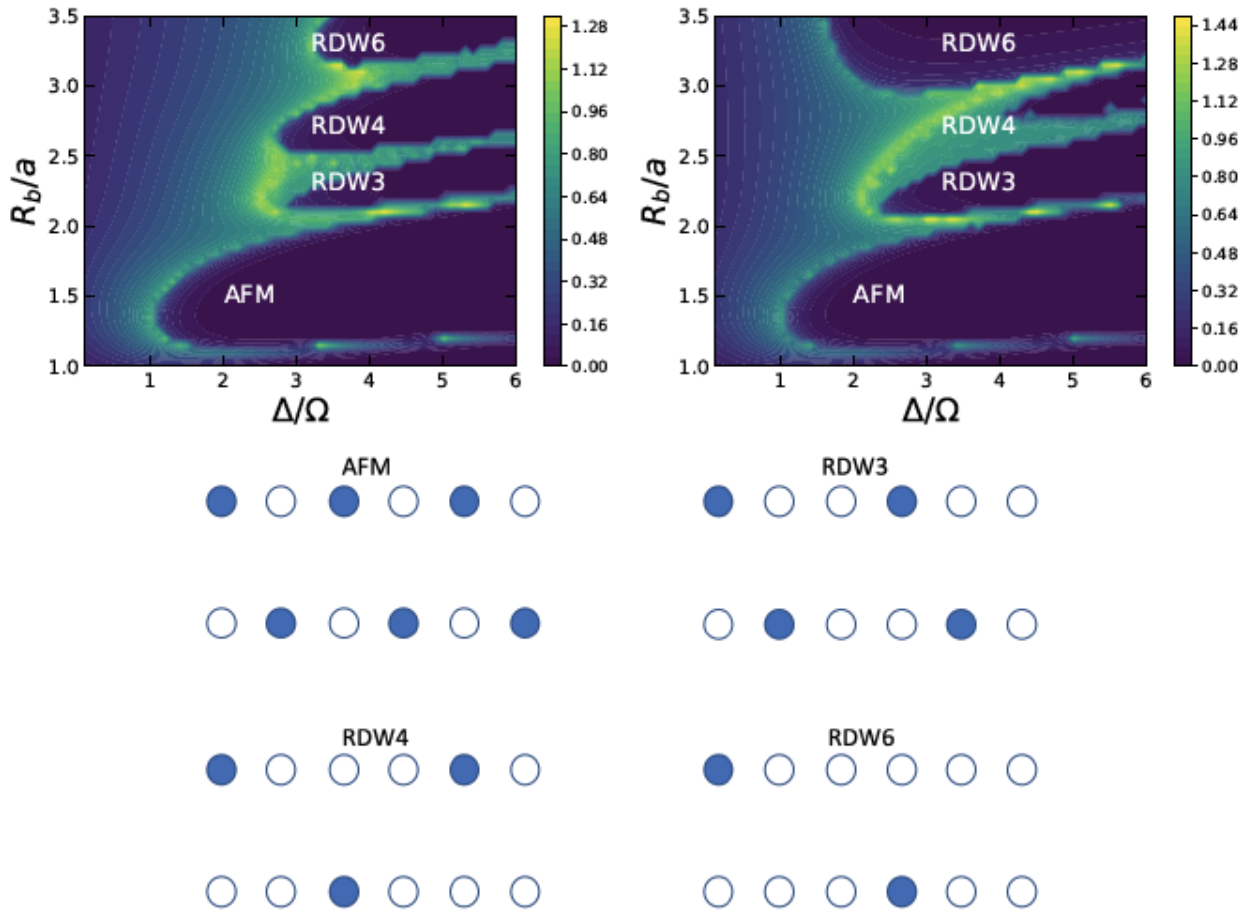

Figure 14: Ground-state phase diagram for the two-leg Rydberg ladder with $dx = dy/2$. Upper left: the number of rungs $L = 144$, retaining interactions between rungs separated by up to twenty lattice units (dx). Upper right: $L = 288$, retaining interactions between rungs separated by up to two lattice units.

Phase diagram for a two-leg ladder (Jin Zhang)

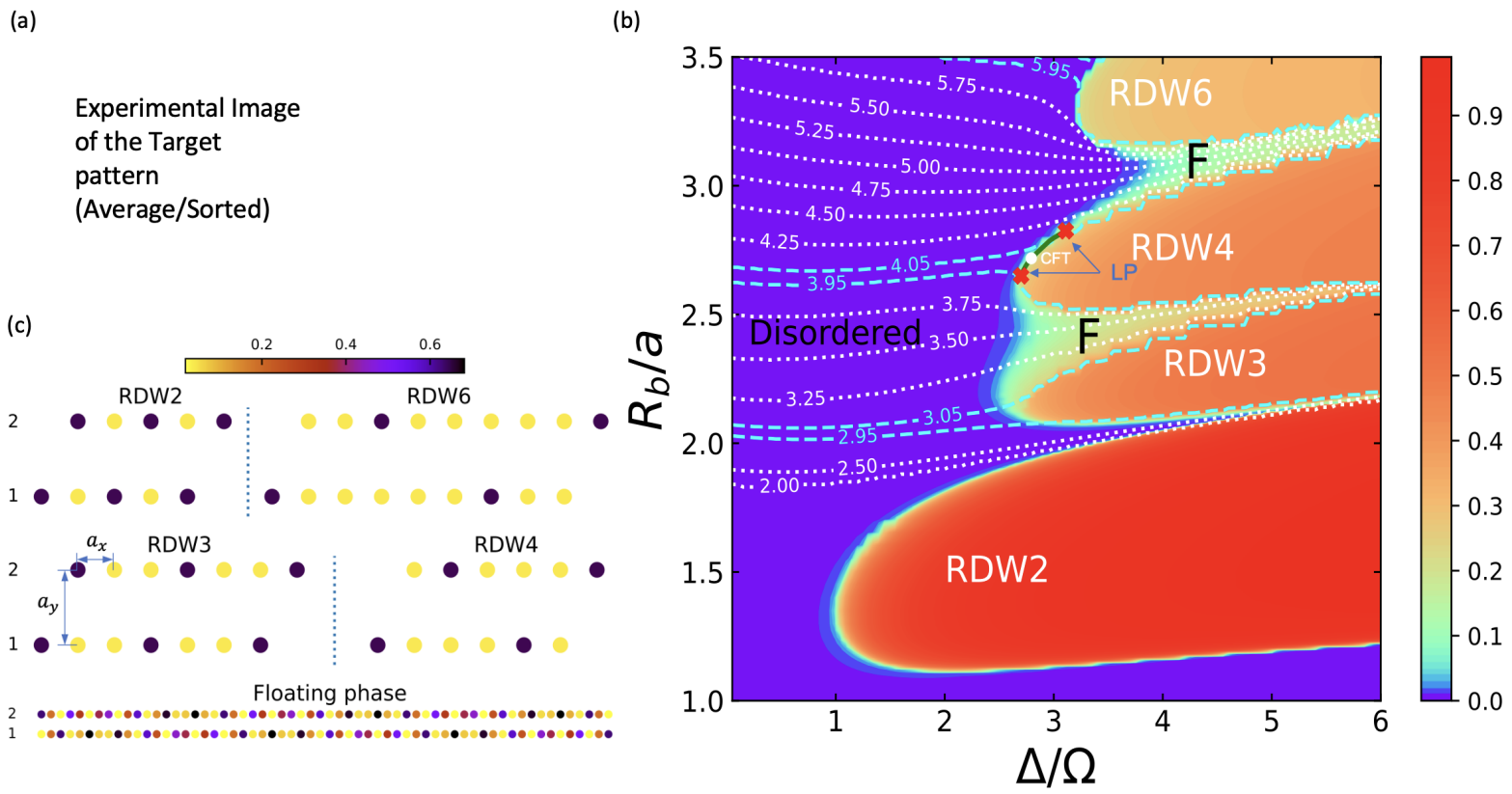

Figure: (a) Experimental Image of the pattern (average/sorted). (b) Ground-state phase diagram for the two-leg ladder of Rydberg atoms with lattice spacing $a_y = 2a_x = 2a$. The structure factor as a function of wave length $p = 2\pi/k$ is calculated. The color depth and the dotted lines represent the peak height and the peak position of the structure factor, respectively.

Experimental implementation (S. Cantu, QuEra)

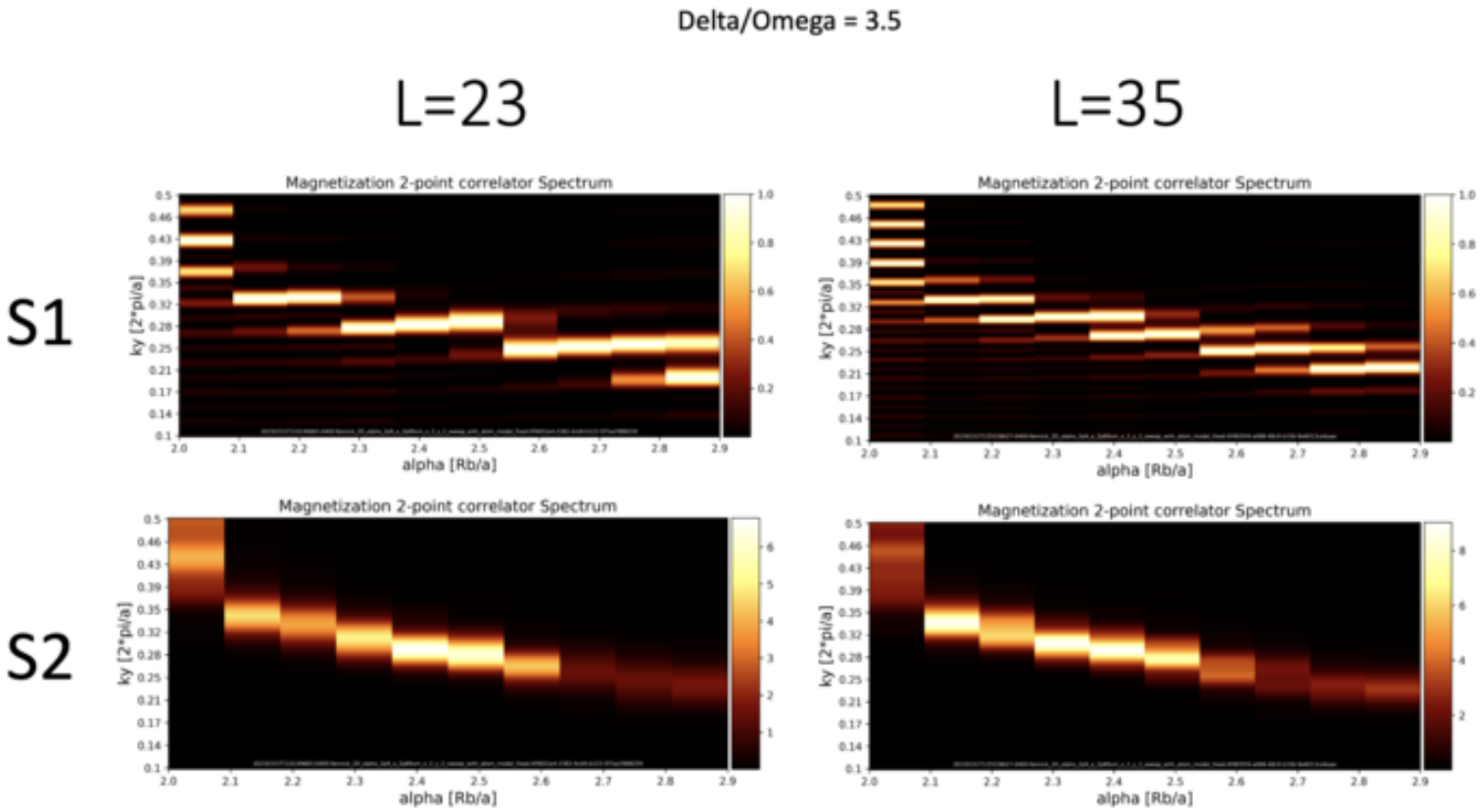

Interpolation among Z_q clock models

Leon Hostetler, Jin Zhang , Ryo Sakai , Judah Unmuth-Yockey , Alexei Bazavov , and YM; arXiv:2105.10450, PRD 104 054505.

- $O(2)$ model with Symm. breaking : $\Delta S = \gamma \sum_x \cos(q\varphi_x)$
- $\gamma \to \infty$: $\varphi = \frac{2\pi k}{q}$ $k = 0, 1, .., \lfloor q \rfloor$
- Integer q: Z_q symmetry
- Non-integer q: Z_2 symmetry
- Phase diagram: see right panel

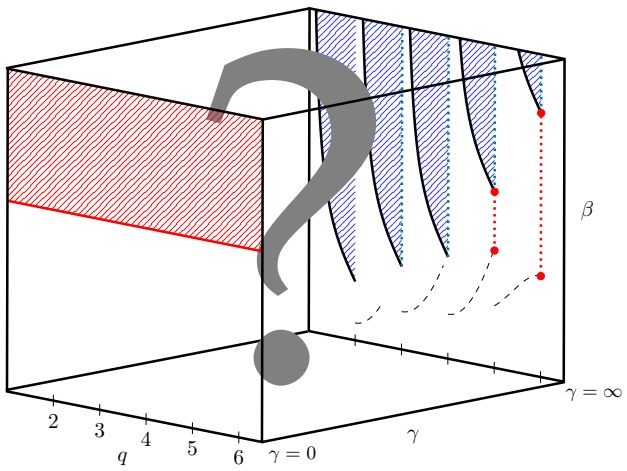

Implementation with Rydberg arrays?

A. Keesling, .., M. Lukin et al. Nature 568: 1D array of ^{87}Rb atoms evenly separated by a controllable distance, homogeneously coupled to the excited Rydberg state $|r\rangle$ with detuning Δ.

$$H = \frac{\Omega}{2} \sum_i (|g_i\rangle\langle r_i| + |r_i\rangle\langle g_i|) - \Delta \sum_i n_i + \sum_{i<j} V_{ij} n_i n_j$$

For $R_b/a \simeq q$ integer and Δ large enough: Z_q ordering.

More numerical work at finite γ

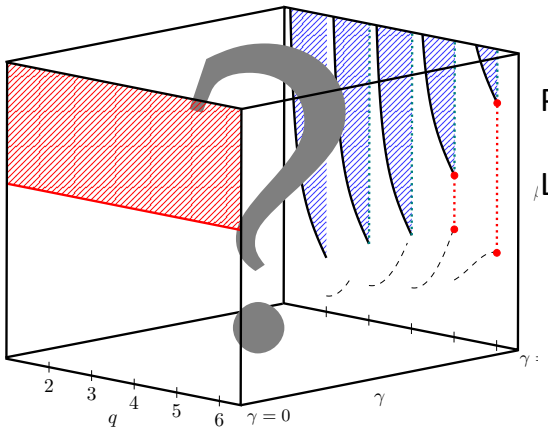

Phase diagram with symmetry breaking (numerical work by Leon Hostetler and Ryo Sakai)

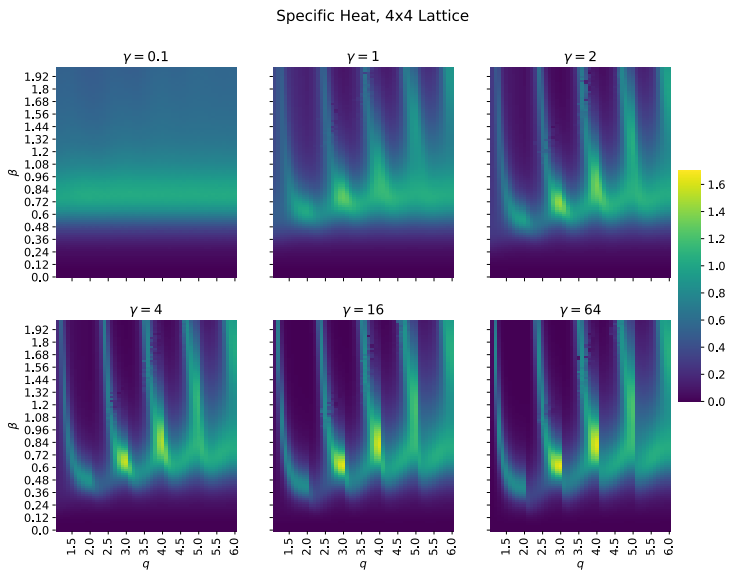

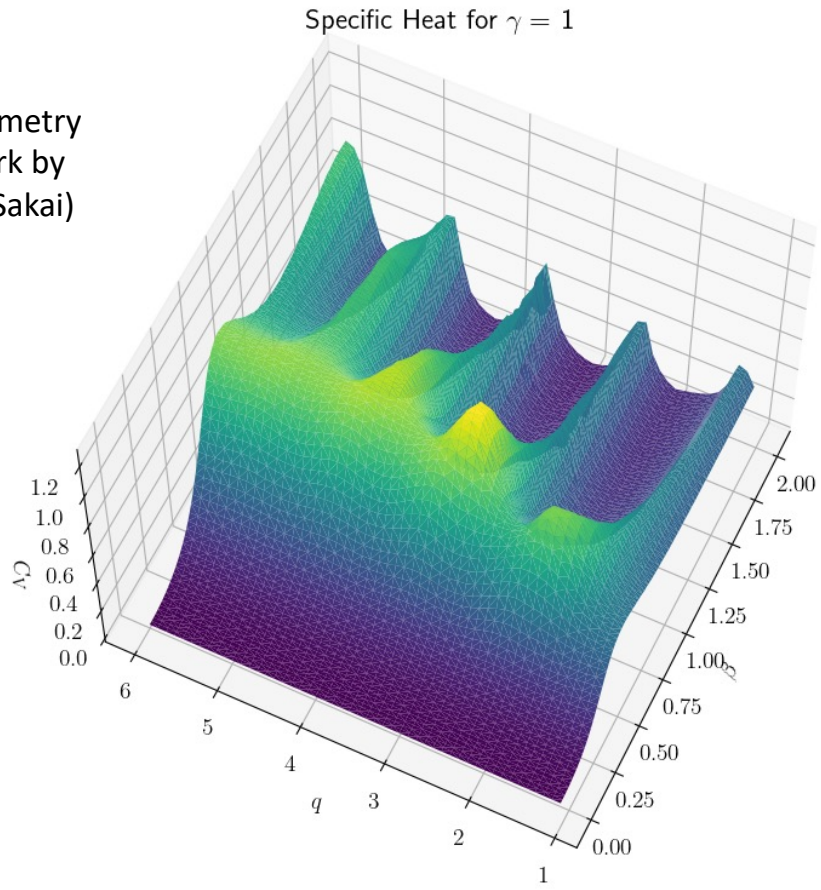

Pythia hadronization (with K. Heitritter and S. Mrenna, 2212.02476))

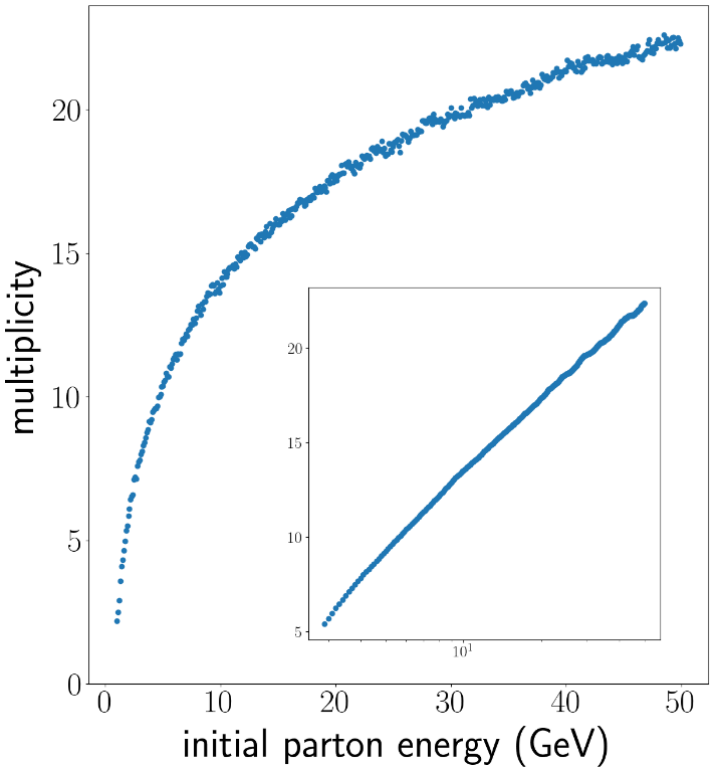

Figure: Hadron multiplicity predictions with default pythia hadronization from an initial $u\bar{u}$ pair. A primary goal for a hadronization model based on Rydberg atoms is to achieve a similar logarithmic behavior. Inset depicts the same data with a logarithmic x-axis and smoothing applied.

Pythia tutorial by K. Heitritter (kenny@qbraid.com)

Hadronization:

Lund String Fragmentation Model

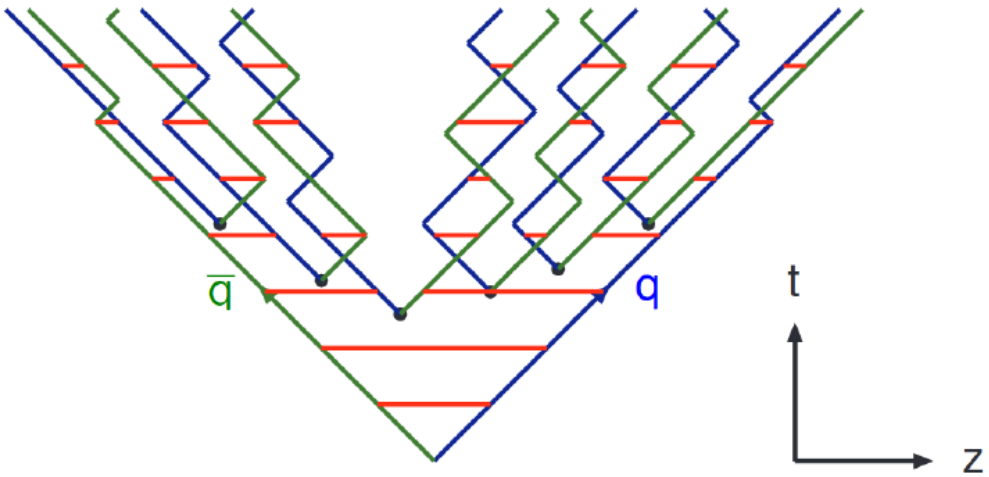

Note: for QIS work related to parton showers (before hadronization, not discussed here) see C. Bauer, Z. Davoudi et al., arXiv:2204.03381, PRX Quantum 4 (2023) 2, 027001

Fragmentation with a two-leg ladder

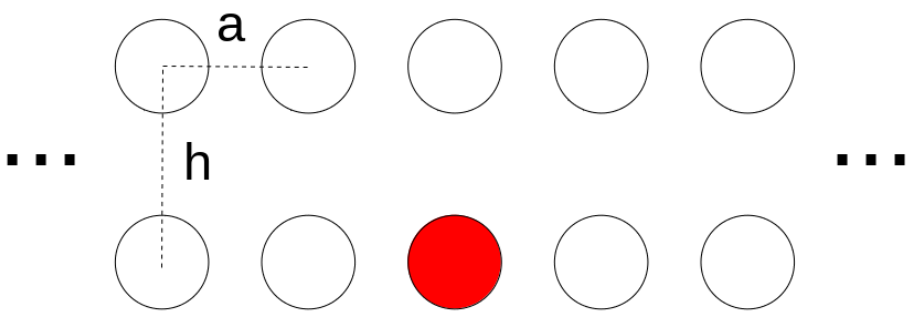

Figure: Two-leg ladder arrangement of Rydberg atoms where h is the inter-rung spacing and a is the outer-rung (lattice) spacing. The ladder can be specified by an inverse aspect ratio $\rho = h/a$, and we work with $\rho = 2$ unless otherwise specified, whereas previous studies (YM PRD 104) have focused on $\rho \sim 0.4$. The red circle represents an excited atom, while the white circles correspond to ground states. Staggered interpretation (below).

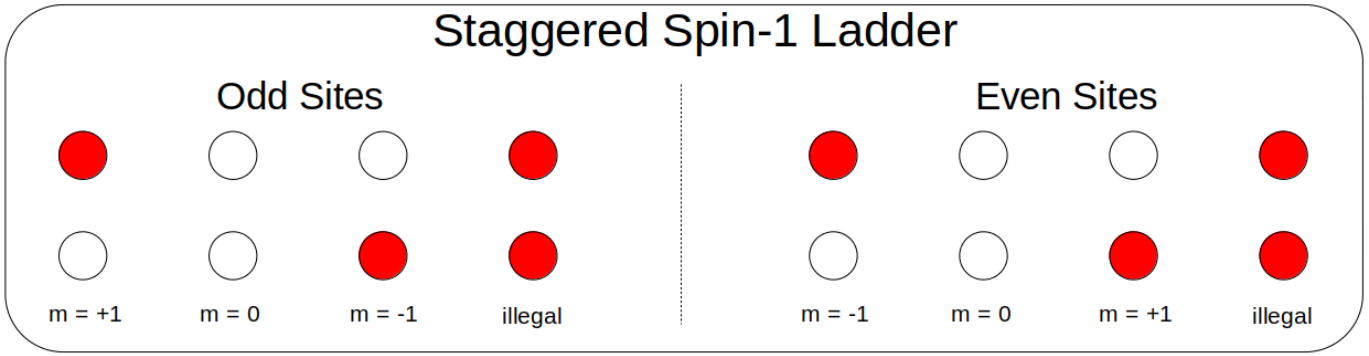

Evolution of particle-antiparticle state (K. Heitritter)

Each column displays the field evolution (a-c) for $R_b/a = 2.173$ and variable Δ/Ω increasing toward the right. For $\Delta/\Omega = 2.0$ (a), the initial field spreads nearly ballistically. As Δ/Ω is increased, the initial field spreads less readily and tends to form greater relative field densities at or close to the central site. It may be possible to interpret the initial excitation as having a higher (lower) energy for lower (higher) Δ/Ω.

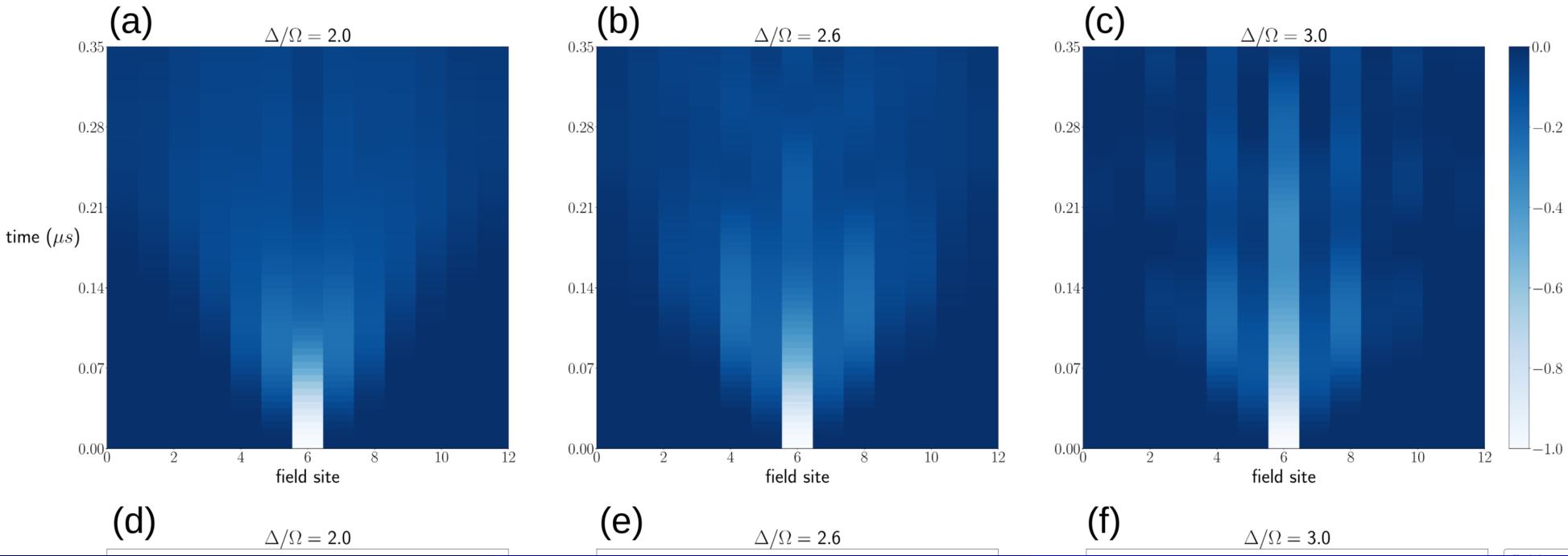

Maximal entropy, K. Heitritter (2212.02476)

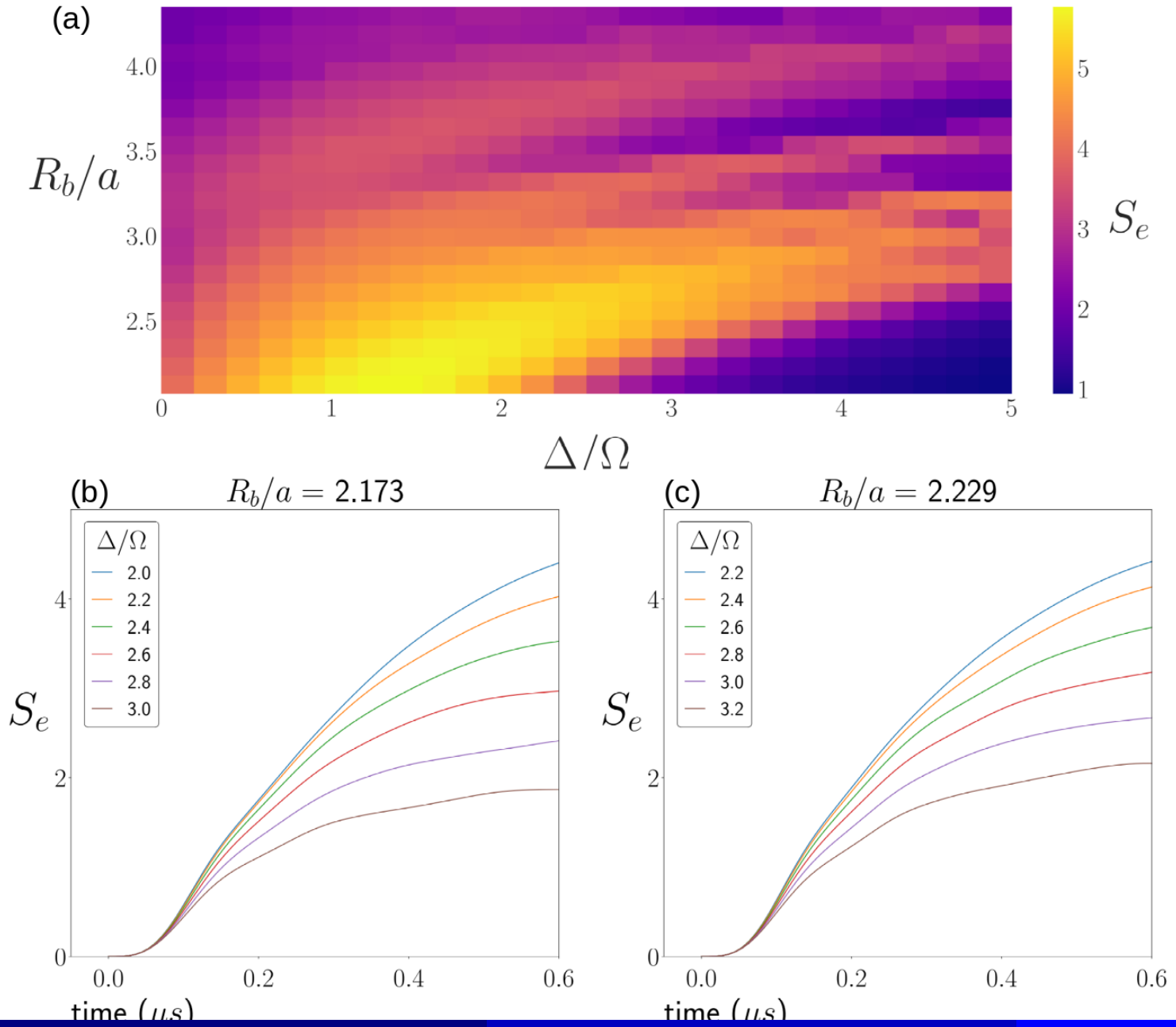

Hadron Multiplicity (K. Heitritter, 2212.02476)

1. Pythia produces parton-level configurations that are organized into color singlets of strings with (usually) quark-antiquark endpoints. The quark and antiquark pair can be boosted to their rest frame with equal and opposite three-momentum.
2. A linear interpolating function translates the energy of the quark-antiquark pair into the global detuning of the initial string configuration on the Rydberg simulator. Energy of the string is set by the Rydberg Hamiltonian and therefore lower (higher) detuning corresponds to higher (lower) energy of the initial state.
3. The string state is prepared on the ladder configuration using local detuning and an adiabatic ramping procedure.
4. The string state is subjected to constant global Rabi flipping and detuning up until excitations reach the lattice boundary. At this time (t_f), the system state is measured. For the 13-rung ladder, this time is set to $t_f = 0.35\ \mu s$.
5. The measured state is post-processed according to steps explained on the next slide

The measured state is post-processed according to the following steps:

1. The staggered spin-1 mapping transforms the ladder into the field representation. The measured state now appears as a number of strings, each with length ≥ 1.
2. The initial string energy is fractionally distributed to the measured strings such that the assigned energies are proportional to the string lengths.
3. The strings are converted to quark-antiquark pairs (mesons) separated by their corresponding string lengths using Gauss' law .
4. Each meson is assigned a velocity by calculating the average velocity of its constituent quark-antiquark pair with respect to the initial string configuration.
5. Each meson is assigned a mass using the previously calculated energy and velocity as inputs to the relativistic energy-mass relation.

Hadron Multiplicity (graph by K. Heitritter, 2212.02476)

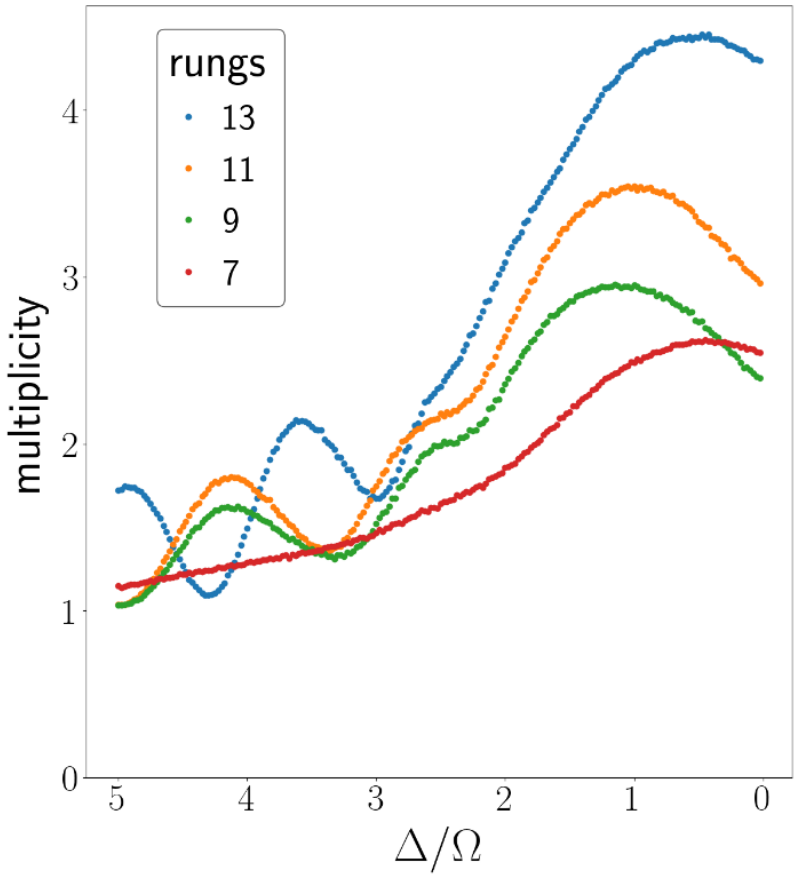

Figure: Hadron multiplicity output of the Rydberg hadronization model for $R_b/a = 2.173$. Δ/Ω is plotted in decreasing order, since smaller values seem to be interpretable as having lower initial system energy and vice versa. The scaling is clearly not logarithmic as for pythia in but does display a monotonic increase in multiplicity for $\Delta/\Omega \in [2, 3]$, which displayed confining-like

Other work with Rydberg atoms

- F. M. Surace, P. P. Mazza, G. Giudici, A. Lerose, A. Gambassi, and M. Dalmonte, Phys. Rev. X 10, 021041 (2020).
- A. Celi, B. Vermersch, O. Viyuela, H. Pichler, M. D. Lukin, and P. Zoller, Phys. Rev. X 10, 021057 (2020).
- S. Notarnicola, M. Collura, and S. Montangero, Phys. Rev. Research 2, 013288 (2020).
- Pierre Fromholz, Mikheil Tsitsishvili, Matteo Votto, Marcello Dalmonte, Alexander Nersesyan, Titas Chanda, Phys. Rev. B 106, 155411 (2022)
- Daniel Gonzalez-Cuadra, Torsten V. Zache, Jose Carrasco, Barbara Kraus, Peter Zoller, Phys. Rev. Lett. 129, 160501 (2022)
- For more refs. see: C. Bauer, Z. Davoudi et al., arXiv:2204.03381, PRX Quantum 4 (2023) 2, 027001

Conclusions

- QC/QIS in HEP and NP: big goals with many intermediate steps
- Tensor Lattice Field Theory (TLFT): generic tool to discretize path integral formulations of lattice model with compact variables
- Truncations preserve symmetries
- TRG (blocking), pert. theory are “friendly competitors" to QC
- TRG: gauge-invariant approach for gauge theories.
- We have proposed a ladder-shaped CARA with two (or three) atoms for a single spin-1.
- Matching between simulator and target model should be understood in the continuum limit (universal behavior).
- Approximate implementations with AWS/QuEra (ongoing)
- Simulators have interesting features beyond our target model.
- Progress with hybrid hadronization
- Thanks for listening!
- For questions, email: yannick-meurice@uiowa.edu .

Thanks for listening!

GC=0.3; st=2; $sth = 1.5$; T=1.5

Figure: Isingized version of Emmy Noether

Building blocks of spin-1 simulators (PRD104)

- One spin-1 with two atoms:
  $H^{2R} = -\Delta(n_{+1}+n_{-1}) + V_0 n_{+1} n_{-1} + \frac{\Omega}{2}\sum_{\pm 1}(|g_{\pm 1}\rangle\langle r_{\pm 1}| + |r_{\pm 1}\rangle\langle g_{\pm 1}|)$
- Coupling two spin-1 as above (four atoms):

$$H^{4R} = H_L^{2R} + H_R^{2R} + V_1(n_{+1L}n_{-1R} + n_{-1L}n_{+1R}) + V_2(n_{+1L}n_{+1R} + n_{-1L}n_{-1R})$$

- One spin-1 with three atoms:
  $H^{3R} = -\Delta_0 n_0 - \Delta\sum_{j=0,\pm 1} n_j + V_0(n_0 n_{+1} + n_0 n_{-1}) + V_0' n_{+1} n_{-1} + \frac{\Omega}{2}\sum_{j=0,\pm 1}(|g_j\rangle\langle r_j| + |r_j\rangle\langle g_j|)$
  Note: Δ_0 is an inhomogeneous detuning that should become experimentally possible soon.
- Coupling two spin-1 as above (six atoms):

$$H^{6R} = H_L^{3R} + H_R^{3R} + V_1(n_{+1L}n_{-1R} + n_{-1L}n_{+1R}) + V_2(n_{0L}(n_{+1R} + n_{-1R})) + V_2((n_{+1L} + n_{-1L})n_{0R}) + V_3(n_{+1L}n_{+1R} + n_{-1L}n_{-1R})$$

Critical behavior of Spin truncations in the $O(2)$ limit

with Jin Zhang and Shan-Wen Tsai PRB 103 245137

$\hat{H}_{charge} = \frac{Y}{2}\sum_{l=1}^{L+1}(\hat{S}_l^z)^2 - \frac{X}{2}\sum_{i=1}^{L}(\hat{U}_l^+\hat{U}_{l+1}^- + \hat{U}_l^-\hat{U}_{l+1}^+)$

Energy gaps $\Delta E_{V=\infty}$ for spin truncations $S = 1, 2, 3, 4$ (by J. Zhang).

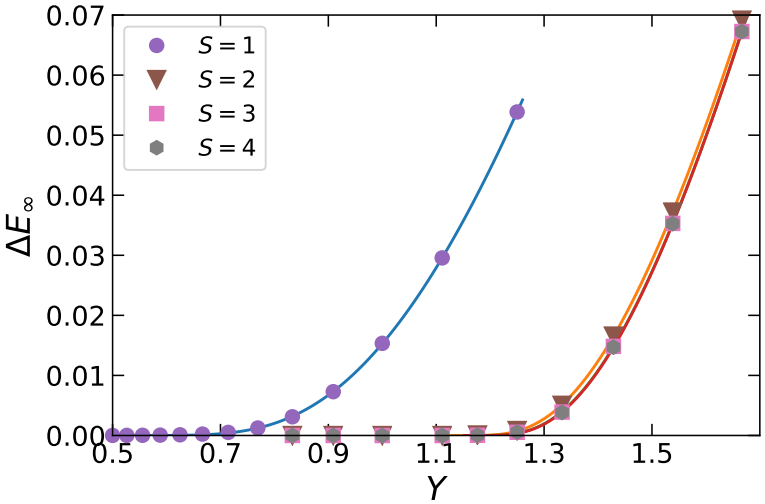

Fits:

- $S \geq 2$: $A\exp(-b/\sqrt{Y - Y_c})$ (regular KT)
- $S = 1$: $A\sqrt{Y - Y_c}\exp[-b/(Y - Y_c)]$ ($SU(2)$ symmetry; KT separatrix)

- $Y_c = 0.350666928(2)$ for $S = 1$; $1.101304(6)$ for $S = 2$; ... using level crossing spectroscopy.
- The dual field representation is gapped at finite S.

Tensors as computational building blocks

- The partition functions are traces of product of tensors
- Observables can be calculated by introducing “impure" tensors
- Tensors are local
- They contain all the information about the model, its dimension and symmetries (universality)
- Most lattice models have a tensor reformulations
- They can be coarse-grained exactly
- RG procedure require truncations (this is the hard part)
- The space of tensors is easier to handle than the space of interactions
- Tensors can be used to build quantum circuits